PILOT BASED CHANNEL ESTIMATION FOR 3GPP LTE DOWNLINK

by

ANKIT ASHOK AGARWAL

Presented to the Faculty of the Graduate School of

The University of Texas at Arlington in Partial Fulfillment

of the Requirements

for the Degree of

MASTER OF SCIENCE IN ELECTRICAL ENGINEERING

THE UNIVERSITY OF TEXAS AT ARLINGTON

December 2011

ACKNOWLEDGEMENTS

First and foremost, I would like to thank my supervisor Dr. Q. Liang for his continued guidance, valuable suggestions and support during the course of my thesis work. I would also like to thank Dr. S. Gibbs and Dr. S. Tjuatja for taking time to serve on my committee.

I sincerely thank my parents and my family for their love, blessings, support and encouragement throughout my life.

Lastly, I would like to thank all my friends and colleagues who have supported me throughout my Master's Degree program at UTA.

November 18, 2011

ABSTRACT

PILOT BASED CHANNEL ESTIMATION FOR 3GPP LTE DOWNLINK

Ankit Ashok Agarwal, M.S.

The University of Texas at Arlington, 2011

Supervising Professor: Qilian Liang

Channel estimation is an important part for the design of receivers in mobile communication systems. In order to recover the transmitted information correctly, the effect of the channel on the transmitted signal must be correctly estimated. In this thesis, the pilot based channel estimation algorithms for 3GPP LTE downlink is studied.

Channel estimation algorithms such as Least Square (LS), Minimum Mean Square Error (MMSE) and Modified MMSE (M-MMSE) channel estimation algorithm have been evaluated for LTE downlink 5 MHz bandwidth configuration. The performance of these algorithms for Block type and Comb type pilot arrangement has been measured in terms of Bit Error Rate (BER). For Comb type pilot arrangement, the performance of Linear Interpolation (LI), Spline Cubic Interpolation (SCI) and Low Pass Interpolation (LPI) methods have been compared. Though higher order interpolation is used for better interpolation accuracy, the improvement in performance is not proven for all cases and for some cases Linear Interpolation can give better performance. For cases when the subcarrier spacing is very small compared to the coherence bandwidth which is a result of small delay spread, Linear Interpolation can give better performance in terms of BER. The ITU outdoor to indoor and pedestrian test environment channel model A, which has a small R.M.S. delay spread of 45 ns, has been used for all

simulations. The performance of Comb type pilot arrangement with different pilot spacing has also been compared.

TABLE OF CONTENTS

LIST OF ILLUSTRATIONS

Figure Page

LIST OF TABLES

Table Page

CHAPTER 1

INTRODUCTION

1.1 Background

Over the last few decades, due to the increasing demand for high speed data and widespread network access in mobile communications, there has been tremendous ongoing research in the field of cellular communications which has resulted in achieving significant developments. The user's demands for high quality wireless communication with higher data rates have been constantly increasing. With limited bandwidth resources and the rapidly growing numbers of users it became necessary to adopt new advanced technologies to meet the current increasing demands for higher data rates. The use of novel technologies like Orthogonal Frequency Division Multiplexing (OFDM) and Multiple Input Multiple Output (MIMO) systems significantly improved the spectrum efficiency of the system and provided high data rates which resulted in a higher capacity. The use of the two technologies helped to enhance the performance of the current wireless communication systems.

With increasing competition among major telecommunication companies and improvements in the technologies, there has been an incredible reduction in the charges imposed by the telecommunication companies. Users now expect higher quality communication services at even lower costs. Thus new systems must be designed with cheaper development, installation and maintenance cost along with providing superior performance which significantly adds to the overall complexity of the system.

Long Term Evolution (LTE) is that next step and is aimed at providing substantial performance enhancement at reduced cost. The 3rd Generation Partnership Project (3GPP) Long Term Evolution (LTE) represents a major advancement in cellular technology and marks

the evolutionary move from third generation of mobile communication (UMTS) to fourth generation mobile technology. LTE is the first cellular communication system supporting packet optimized radio access technology with high data rates and low latencies.

The 3GPP started work on Long Term Evolution in release 8 of the 3GPP UMTS specifications after completion of its feasibility studies. A summary of the release 8 specifications with description of targets can be found in [1]. This release was mainly focused on further improvements on High Speed Packet Access (HSPA) along with the specification of LTE and System Architecture Evolution (SAE). Currently work is in progress for the enhancement of LTE which is termed LTE-Advanced (LTE-A). Table 1.1 provides a comprehensive summary of the evolutionary trend of the 3GPP group technical specifications.

Table 1.1 Technical Specifications Published by the 3GPP Group

Release	Specification	Date
Release 99	W-CDMA	1999
Release 4	1.28 Mcps TDD	2001
Release 5	HSDPA, IMS	2002
Release 6	HSUPA, MBMS, IMS+	2004
Release 7	HSPA+ (MIMO, HOM)	2006
Release 8	LTE, SAE	2008
Release 9	Small LTE,SAE Enhancements	2009
Release 10	LTE-Advanced	2010

1.2 LTE Key Features

The key features or advantages of LTE are:

- Supports scalable bandwidths of 1.25, 2.5, 5, 10 and 20 MHz in order to allow flexible technology to coexist with each other
- Increased peak data rates up to 100 Mbps in Downlink and 50 Mbps in Uplink within a 20 MHz system bandwidth
- Reduced Control plane latency to less than 100 ms and User plane latency to less than 10 ms
- Mobility is optimized for low speeds but maintain links and provides interactive real time services at speeds up to 350 km/hr
- Support multiple antenna configurations both in Downlink and Uplink so as to improve the system performance by using transmit diversity, spatial multiplexing and beam forming techniques
- Coverage with full performance up to 5 km, slight degradation up to 30 km coverage and support of coverage of up to 100 km.
- Reduced integration cost and power consumption. One of the key features of LTE is multi-vendor RAN or self-optimizing networks (SON) which reduces operational expenditure (OPEX) and provides low costs per bit.
- All IP Network based to support different types of services with different Quality of Service (QoS) and to provide easy integration with other communication networks.
- Increased spectrum efficiency up to 3 to 4 times HSDPA Rel. 6 in Downlink and up to 2 to 3 times HSUPA Rel. 6 in the Uplink
- LTE provides greater improvement in overall performance and efficiency through the use of OFDM technology for the air interface rather than WCDMA based UTRAN and HSPA system

1.3 Thesis Outline

The effect of the channel on the transmitted signal must be correctly estimated in order to recover the transmitted information correctly. The quality of the system transmission is directly determined by the accuracy of the channel estimation. In this thesis, the pilot based channel estimation algorithms for 3GPP LTE downlink is studied.

The first chapter gives an introduction to LTE and describes the background of this technology and its role in the present mobile communication systems. The second chapter gives an overview of the LTE downlink physical layer. It describes the OFDM system model, LTE downlink frame structure, resource structure, bandwidth configuration, physical channels and the reference signals. The third chapter describes the wireless radio propagation models, multipath fading and time varying statistical properties of the wireless channel. In the fourth chapter, the different pilot arrangement for channel estimation is described. Channel estimation algorithms such as Least Square (LS), Minimum Mean Square Error (MMSE) and Modified MMSE (M-MMSE) channel estimation algorithm have been evaluated for LTE downlink 5 MHz bandwidth configuration. In the fifth chapter, the performance of these algorithms for Block type and Comb type pilot arrangement has been measured in terms of Bit Error Rate (BER). For Comb type pilot arrangement, the performance of Linear Interpolation (LI), Spline Cubic Interpolation (SCI) and Low Pass Interpolation (LPI) methods have been compared. Also the effect of different pilot subcarrier spacing has been compared for Comb type pilot arrangement. All the simulations are performed using MATLAB. The last chapter focuses on the conclusions and future works.

CHAPTER 2

LTE PHYSICAL LAYER

2.1 Introduction

The LTE Physical Layer is a highly efficient means of conveying both data and control information between an enhanced base station (eNodeB) and mobile user equipment (UE). The LTE Physical Layer is based on Orthogonal Frequency Division Multiple Access (OFDMA) for the downlink (DL) and Single Carrier - Frequency Division Multiple Access (SC-FDMA) for the uplink (UL). The LTE Physical Layer also employs MIMO data transmission techniques for increasing the capacity as well as the overall performance of the system. LTE supports both Frequency Division Duplex (FDD) and Time Division Duplex (TDD) modes and each one has its own frame structure.

The LTE Physical Layer consists of the physical channels and the physical signals which are defined in [2]. The physical channels are responsible for carrying data from higher layers including control data, scheduling and user payload. The physical signals are used for system synchronization, cell identification and radio channel estimation.

The types of downlink physical channels are Physical Downlink Shared Channel (PDSCH), Physical Broadcast Channel (PBCH), Physical Multicast Channel (PMCH), Physical Control Format Indicator Channel (PCFICH), Physical Downlink Control Channel (PDCCH) and Physical Hybrid ARQ Indicator Channel (PHICH). The types of uplink physical channels are Physical Random Access Channel (PRACH), Physical Uplink Control Channel (PUCCH) and Physical Uplink Shared Channel (PUSCH). There are two types of physical signals, namely the Reference signal and the Synchronization signal.

2.2 OFDM System Model

The Orthogonal Frequency Division Multiplexing (OFDM) transmission scheme is a type of multichannel system similar to the Frequency Division Multiplexing (FDM) transmission scheme as it also uses multiple sub-carriers. However in OFDM, the sub-carriers are closely spaced to each other without causing interference, thus removing the required guard bands between adjacent sub-carriers. This is possible because the sub-carriers or the frequencies are orthogonal i.e. the peak of one sub-carrier coincides with the null of an adjacent sub-carrier. The time-frequency representation of the OFDM signal is shown in figure 2.1.

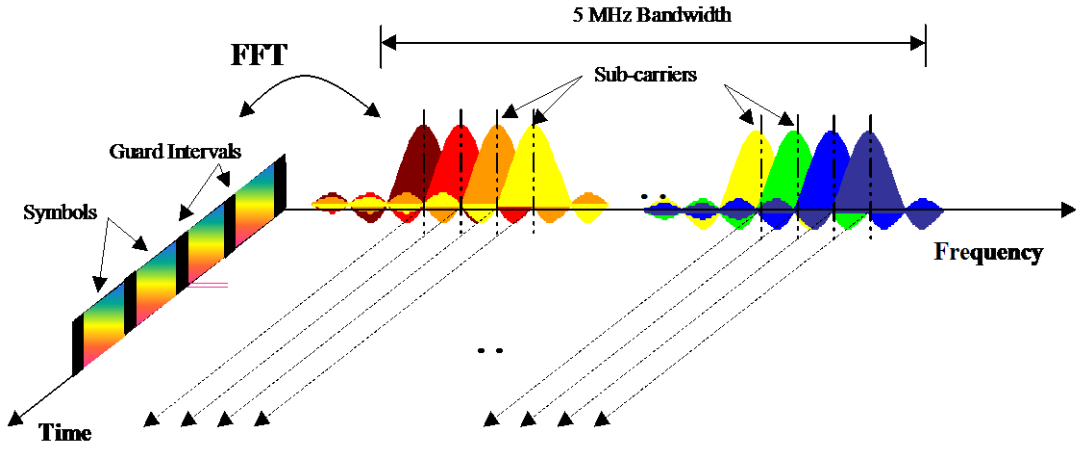

Figure 2.1 Time-Frequency Representation of an OFDM Signal [17]

Unlike single carrier systems, OFDM communication systems do not rely on increased symbol rates in order to achieve higher data rates. This makes the task of managing ISI much simpler. In OFDM system, a very high rate data stream is divided into multiple parallel low rate data streams. Each smaller data stream is then mapped to individual data sub-carrier and modulated using varying levels of PSK or QAM modulation schemes depending on the signal quality. Each OFDM symbol is therefore a linear combination of the instantaneous signals on each of the sub carriers in the channel. Because data is transmitted in parallel rather than

serially, OFDM symbols are generally much longer than symbols on single carrier systems of equivalent data rate.

The advantage of such an OFDM scheme is that it needs less bandwidth than FDM to carry the same amount of information which translates to higher spectral efficiency. To make efficient use of available bandwidth, the sub-carriers are very tightly spaced. Due to the orthogonality among the sub-carriers, there is virtually no inter-carrier interference (ICI) among adjacent sub-carriers. Also, an OFDM system is more resilient in NLOS environment. It can efficiently overcome interference and frequency selective fading caused by multipath because equalizing is done on a subset of sub-carrier instead of a longer single broader carrier. The effect of ISI is suppressed by virtue of a longer symbol period of the parallel OFDM sub-carriers than a single carrier system and the use of a cyclic prefix (CP).

Like all other modulation schemes, OFDM also suffers from some drawbacks. It is susceptible to carrier frequency errors due to either local oscillator offset or Doppler shifts. It also suffers from a large peak to average power ratio (PAPR) due to the in-phase addition of sub-carriers. Since the OFDM symbol is a combination of all of the subcarriers, subcarrier voltages can add in-phase components at some points within the symbol, resulting in very high instantaneous peak power which may be much higher than the average power. The power amplifiers must accommodate these occasional peaks which ultimately results in low efficiency of the power amplifiers. The RF Power Amplifier efficiencies for OFDM signals can be less than 20 percent. To minimize PAPR, LTE employs SC-FDMA in the uplink which exhibits 3-6 dB less PAPR than OFDMA.

2.2.1 OFDM Transmitter

In an OFDM system, the signal to be transmitted is defined in the frequency domain. A serial to parallel (S/P) converter first collects the serial data symbols into a data block S_k of dimension *M*. S_k is given as:

$$S_k = [\, S_k[0], S_k[1], \ldots\ldots, S_k[M-1] \,]^T \quad (2.1)$$

The subscript *k* is an index of an OFDM for the *M* sub-carriers. The *M* parallel data streams are first independently modulated using different modulation schemes like QPSK, 16 QAM, or 64 QAM, resulting in the complex vector X_k given as:

$$X_k = [\, X_k[0], X_k[1], \ldots\ldots, X_k[M-1] \,]^T \quad (2.2)$$

This vector of data symbols is then passed through an Inverse Fast Fourier Transform (IFFT) block which results in a set of *N* complex time domain samples x_k given as:

$$x_k = [\, x_k[0], x_k[1], \ldots\ldots, x_k[N-1] \,]^T \quad (2.3)$$

In a practical OFDM system, the number of processed sub-carriers is greater than the number of modulated sub-carriers i.e. $M \geq N$, with the un-modulated sub-carriers being padded with zeros. Next, a guard period is created at the beginning of each OFDM symbol to eliminate the impact of ISI caused by multipath propagation. The guard period is obtained by adding a Cyclic Prefix (CP) at the beginning of the symbol x_k. The CP is generated by appending the last *G* samples of the IFFT output at the beginning of the symbol x_k. The resulting time domain OFDM symbol is given as:

$$[\, x_k[N-G], \ldots\ldots, x_k[N-1], x_k[0], \ldots\ldots, x_k[N-1] \,]^T \quad (2.4)$$

The CP length *G* must be longer than the longest channel impulse response to be supported in order to avoid ISI completely. The CP converts the linear convolution of the channel into a circular one which is suitable for DFT processing. The output of the IFFT is then parallel to serial (P/S) converted for transmission through the frequency selective channel. Figure 2.2 shows the typical block diagram of the OFDM transmitter system [3].

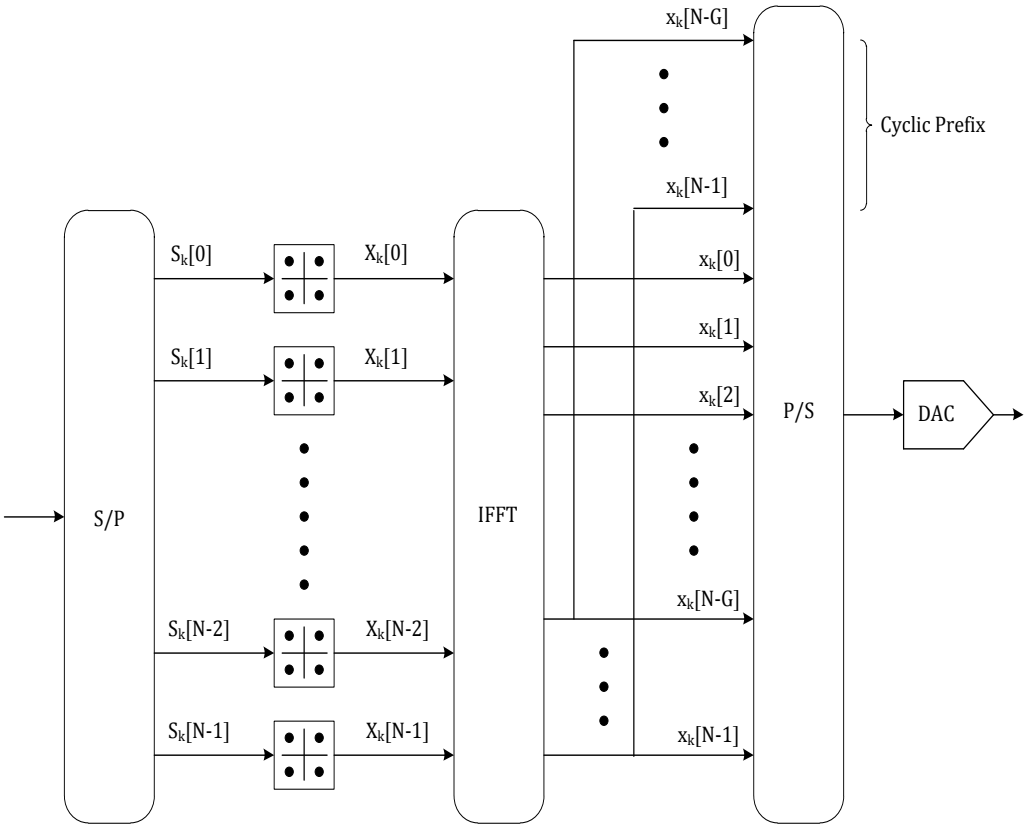

Figure 2.2 OFDM Transmitter

2.2.2 OFDM Receiver

In order to demodulate the OFDM signal at the receiver end, the reverse operations are performed. The serial to parallel converter collects the data symbols first. Then the CP is removed such that only an ISI free block of samples is passed to the DFT. The number of sub-carriers *N* is generally designed to be a power of 2 so that a highly efficient FFT implementation may be used to transform the received signal back to the frequency domain. The modulated subsets of *M* sub-carriers are selected from the *N* parallel streams output from the FFT and further processed by the receiver. Figure 2.3 shows the typical block diagram of the OFDM receiver system [3].

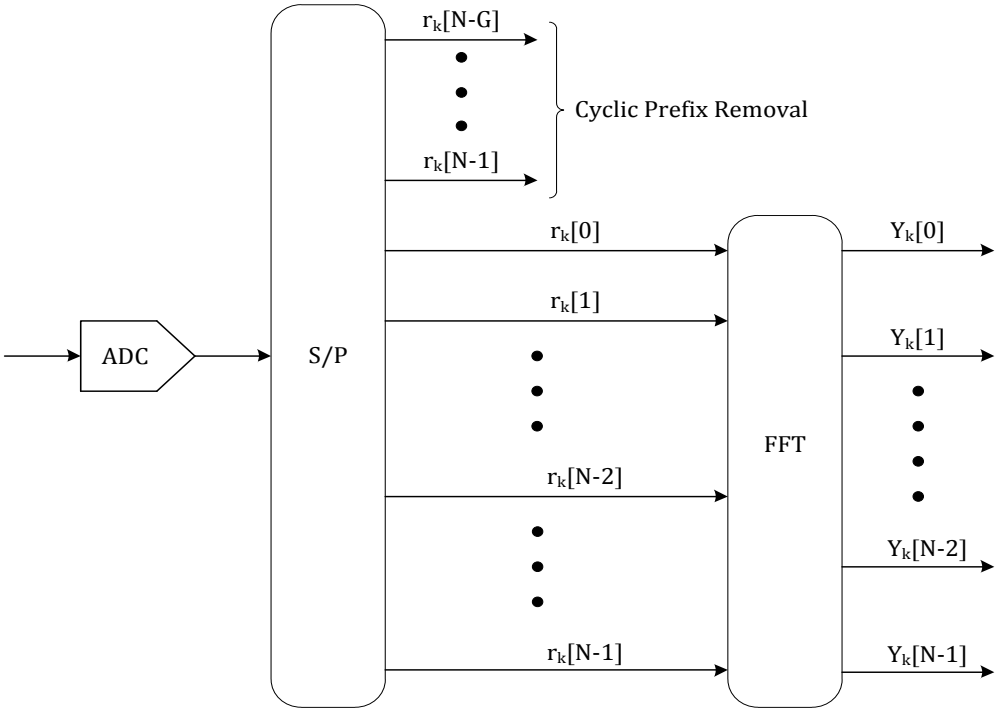

Figure 2.3 OFDM Receiver

2.3 LTE Bandwidth and Resource Configuration

LTE supports scalable bandwidth from 1.25 MHz to 20 MHz and the physical resource block configuration parameters depend on the overall transmission bandwidth of the system. A physical resource block is the smallest element of resource allocation assigned by the base scheduler. For FDD mode, the frame structure is same for both downlink and uplink. The LTE resource configuration for different supportable bandwidth is described in table 2.1.

Depending on the channel delay spread, either a short or long cyclic prefix (CP) is used. When short CP is used, the first OFDM symbol in a slot has slightly longer CP than the remaining six symbols to preserve the slot timing of 0.5 ms. The OFDM symbol length and the CP duration is described in table 2.2. The normal and extended CP duration in absolute terms is described in table 2.3. It is in terms of standard units of time (T_S) which is defined as $T_S =$

$1/(15000 * 2048)$ seconds and it corresponds to the 30.72 MHz sample clock for the 2048 point FFT used with the 20 MHz system bandwidth [2].

Table 2.1 LTE Bandwidth and Resource Configuration

Channel Bandwidth (MHz)	1.25	3	5	10	15	20
Transmission Bandwidth (MHz)	1.08	2.7	4.5	9	13.5	18
Number of Resource Blocks (N_{RB})	6	15	25	50	75	100
Number of occupied sub-carriers	72	180	300	600	900	1200
IFFT (Tx) / FFT (Rx) size	128	256	512	1024	1536	2048
Sample Rate (MHz)	1.92	3.84	7.68	15.36	23.04	30.72
Samples per slot	960	1920	3840	7680	11520	15360
Physical Resource Block Bandwidth	180 kHz					
Sub-carrier Spacing (Δf)	15 kHz					
Sub-frame or slot duration	0.5 ms					

Table 2.2 OFDM Symbol Length and Cyclic Prefix Duration

Channel Bandwidth		1.25	3	5	10	15	20
OFDM symbol per slot (short/long)		7/6					
CP length $\mu sec/samples$	Short	(4.69/9) x6	(4.69/18) x6	(4.69/36) x6	(4.69/72) x6	(4.69/108) x6	(4.69/144) x6
		(5.21/10) x1	(5.21/20) x1	(5.21/40) x1	(5.21/80) x1	(5.21/120) x1	(5.21/160) x1
	Long	16.67/32	16.67/64	16.67/128	16.67/256	16.67/384	16.67/512

Table 2.3 Normal and Extended Cyclic Prefix Duration

Configuration		Cyclic Prefix Length	
		T_S	μsec
Normal CP	Δf = 15 kHz	160 for l = 0	5.21 for l = 0
		144 for l = 1, 2, 3, 4, 5	4.69 for l = 1, 2, 3, 4, 5
Extended CP	Δf = 15 kHz	512	16.67
		1024	33.33

2.4 Frame Structure

LTE supports two types of radio frame structure: Type-1 frame structure for the Frequency Division Duplex (FDD) mode and Type-2 frame structure for the Time Division Duplex (TDD) mode. The LTE frame structures are given in detail in [2].

2.4.1 Type-1 Frame Structure

The Type-1 Frame Structure is relevant for FDD and has radio frame duration of 10 ms duration which consists of 10 sub-frames. Each sub-frame is of length 1 ms and consists of two consecutive slots, each of 0.5 ms duration. Slot consists of either 6 or 7 OFDM symbols, depending on whether the normal or extended cyclic prefix is employed. Thus, type-1 frame structure consists of a total of 20 slots, each of 0.5 ms duration, over a 10 ms frame length. For FDD mode, in each 10 ms frame interval, half of the sub-frames are available for downlink and the other half are available for uplink transmission. The uplink and the downlink transmission are separated in the frequency domain. The Type-1 frame structure is illustrated in figure 2.4.

.

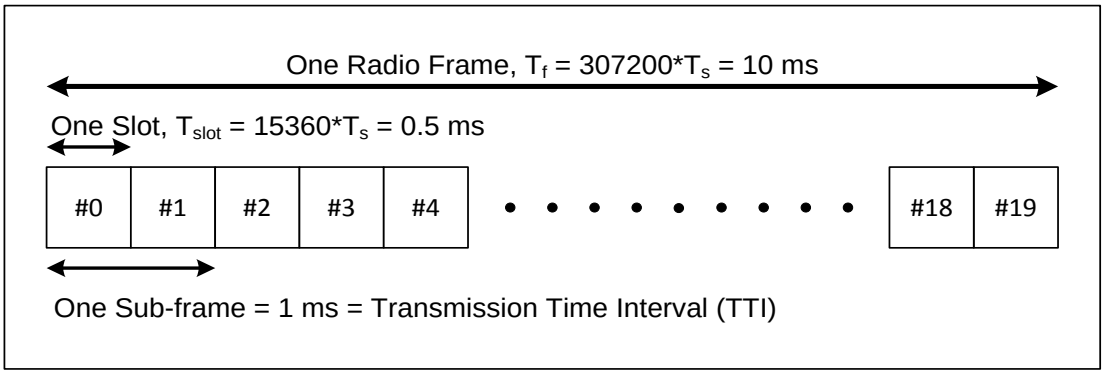

Figure 2.4 Type-1 Frame Structure

2.4.2 Type-2 Frame Structure

The Type-2 Frame Structure is relevant for TDD and also has radio frame duration of 10 ms which consists of two identical half-frames each of 5 ms duration. Each half-frame is further divided into 5 sub-frames, each of 1 ms duration. A sub-frame which is not a special sub-frame consists of two slots of length 0.5 ms. The special sub-frame (S) consists of three fields: Downlink Pilot Time Slot (DwPTS), Guard Period (GP) for TDD operation and Uplink Pilot Time Slot (UpPTS). Uplink-downlink configurations with both 5 ms and 10 ms downlink-to-uplink switch-point periodicity are supported. In case of 5 ms downlink-to-uplink switch-point periodicity, the special sub-frame exists in both half-frames. In case of 10 ms downlink-to-uplink switch-point periodicity, the special sub-frame exists in the first half-frame only. The Type-2 frame structure is illustrated in figure 2.4. Seven uplink downlink configurations are supported with both types (10 ms and 5 ms) of downlink-to-uplink switch-point periodicity. For downlink transmission sub-frames 0, 5 and DwPTS are always reserved. UpPTS and the sub-frame immediately following the special sub-frame are always reserved for uplink communication. The Type-2 frame structure with supporting downlink-uplink configuration is shown in table 2.5 where “U”, “D” and “S” denotes the sub-frames reserved for uplink transmission, downlink transmission and the special sub-frames respectively.

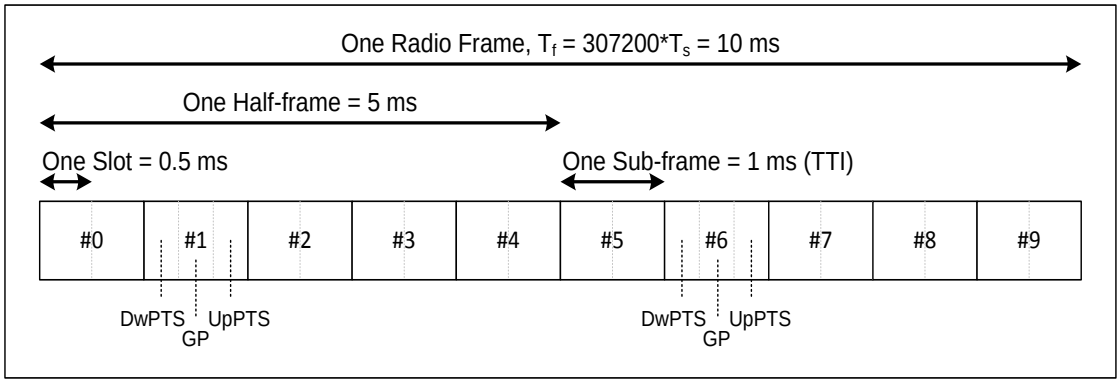

Figure 2.5 Type-2 Frame Structure

Table 2.4 Uplink-Downlink Configuration for LTE TDD

Uplink-Downlink Configuration	DL-to-UL switch-point periodicity	Sub-frame Number									
		0	1	2	3	4	5	6	7	8	9
0	5 ms	D	S	U	U	U	D	S	U	U	U
1	5 ms	D	S	U	U	D	D	S	U	U	D
2	5 ms	D	S	U	D	D	D	S	U	D	D
3	10 ms	D	S	U	U	U	D	D	D	D	D
4	10 ms	D	S	U	U	D	D	D	D	D	D
5	10 ms	D	S	U	D	D	D	D	D	D	D
6	5 ms	D	S	U	U	U	D	U	U	U	D

2.5 Slot Structure and Physical Resource Block

In each slot, the transmitted signal consists of one or several physical resource blocks (PRB) where each individual resource element (RE) corresponds to one OFDM subcarrier during the respective OFDM symbol interval. A physical resource block is defined as the number of OFDM symbols (N_{sym}^{DL}) in each slot in the time domain and the total the number of subcarriers (N_{sc}^{RB}) in each resource block in the frequency domain. In LTE downlink, the subcarrier spacing (Δf) used is of 15 kHz. Thus, each resource block consists of 12 subcarriers

(N_{sc}^{RB}) with 180 kHz bandwidth. The total number of such downlink resource block (N_{RB}^{DL}) is specified by the bandwidth configuration used. The number of OFDM symbols (N_{sym}^{DL}) in each slot is defined by the type of cyclic prefix (CP) used. For normal CP, each slot contains 7 OFDM symbols and for extended CP, 6 OFDM symbols are used. In this thesis work, normal CP with 7 OFDM symbols has been used along with the Type-1 frame structure. The slot structure and the physical resource grid for the 5 MHz bandwidth configuration for LTE downlink is illustrated in figure 2.6.

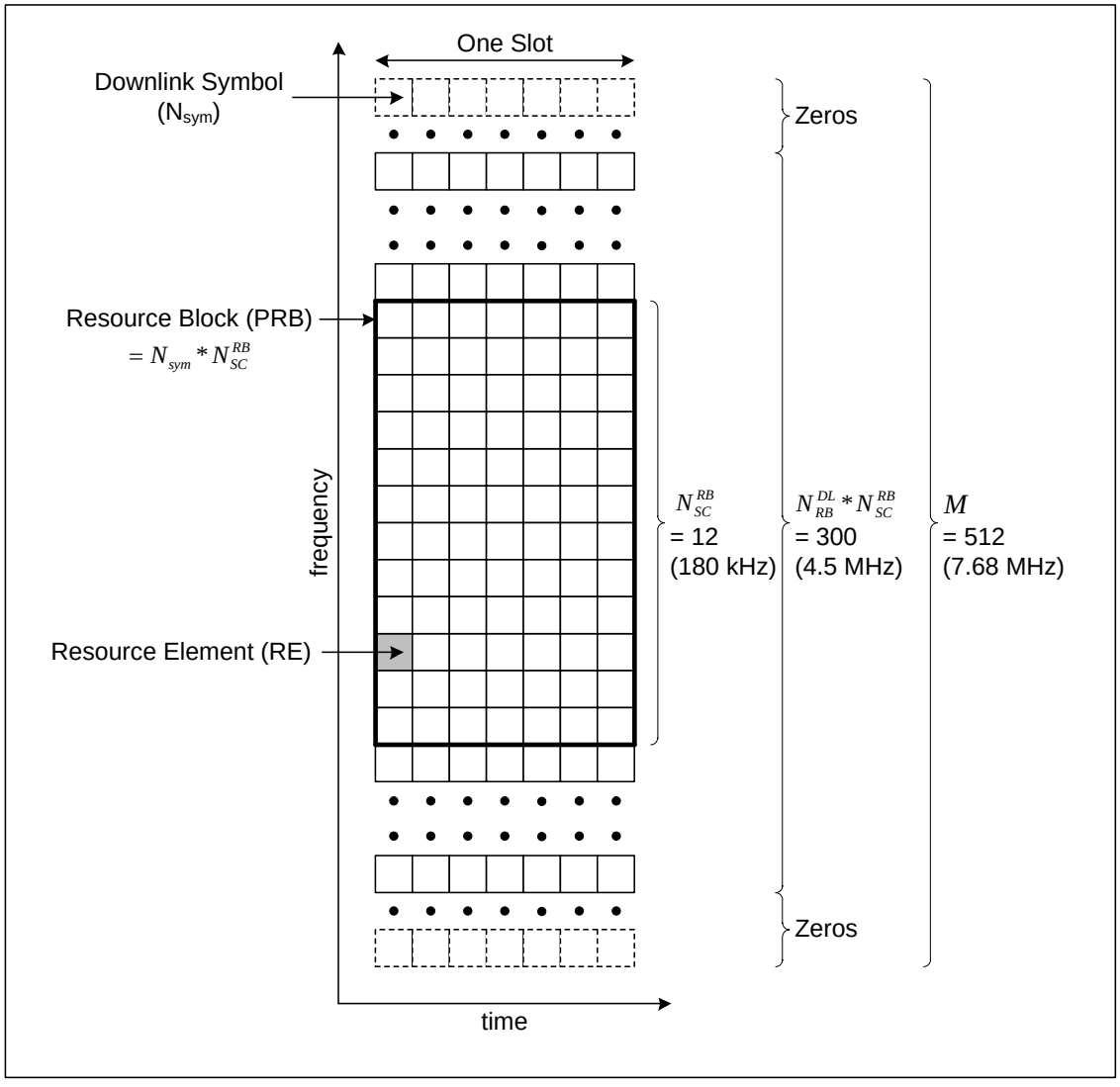

Figure 2.6 Physical Resource Block Structure for LTE Downlink 5 MHz Bandwidth Configuration

2.6 Physical Channels

The LTE air interface comprises of physical channels and physical signals. The physical signals are created in Layer 1 and they are used for system synchronization, cell identification, and radio channel estimation. The physical channels are used to carry data from higher layer including control, scheduling, and user payload.

2.6.1 LTE Downlink Physical Signals

- Primary Synchronization Signal (PSS): It is used for cell search and identification by the user equipment (UE). It carries a part of the cell ID.
- Secondary Synchronization Signal (SSS): It performs the same function as the PSS but carries the remainder of the cell ID.
- Reference Signal (RS): Used for downlink channel estimation.

2.6.2 LTE Downlink Channels

- Physical Downlink Shared Channel (PDSCH): This channel transports data and multimedia (payload) hence it is designed for very high data rates. QPSK, 16-QAM and 64-QAM are suitable modulation techniques that can be employed in this channel.
- Physical Downlink Control Channel (PDCCH): This channel carries control information that is UE-specific e.g. scheduling, ACK/NACK. Therefore, robustness is of main interest than maximum data rate. QPSK is the only available modulation format.
- Common Control Physical Channel (CCPCH): This channel conveys cell-wide control information. The CCPCH is transmitted as close to the center frequency as possible.
- Physical broadcast channel (PBCH): It carries cell-specific/system information.
- Physical multicast channel (PMCH): It is a downlink physical channel that carries the multicast/broadcast information.

- Physical control format indicator channel (PCFICH**)**: It defines the number of PDCCH OFDMA symbols per sub-frame.

2.7 LTE Downlink Reference Signals

In the LTE downlink, for the purpose channel estimation, known reference symbols called pilot symbols or known reference subcarriers called pilot subcarriers are added into time-frequency grid during the OFDM transmission. These reference signals are called LTE Downlink Reference signals. The OFDM transmission in LTE downlink can be described by a two dimensional lattice structure in time and frequency as described in chapter 4. All correlations between the channel coefficients in time as well as frequency domain must be taken into account for accurate channel estimation. Since reference signals are sent only on particular pre-defined resource elements, channel estimates for the data subcarriers must be computed via interpolation techniques. Wiener filter interpolation is the optimal interpolating channel estimator in terms of mean square error for two-dimensional time-frequency interpolation over multiple reference symbols. However, due to the high complexity a combination of two one-dimensional filters are used.

In the time domain, the first and the third last elements of resource grid contains the reference symbols, whereas in frequency domain reference signals are inserted over every six sub-carriers. There is only one reference signal transmitted from each antenna port in the downlink to estimate the channel characteristics. Figure 2.7 shows the reference signal for LTE downlink. In case of multiple antenna schemes, reference signals are mapped on different sub-carries of resource grid for different antennas to avoid interference. Resource elements used to transmit reference signals from one antenna are not reused on the other antenna for data transmission and these places are filled with zeros. For LTE downlink, the different types of reference signals and their allocation is described in [2].

- Cell-specific reference signals (CRS): CRS signals are transmitted in all downlink sub-frames in a cell supporting PDSCH transmission. CRS are defined for subcarrier spacing of 15 kHz only and are transmitted on one or several of antenna ports 0 to 3.
- UE-specific reference signals (DM-RS): UE-specific reference signals are supported for transmission of PDSCH and are transmitted on antenna ports five, seven or eight.
- Positioning reference signals (PRS): PRS are transmitted in resource blocks in downlink sub-frames configured for positioning reference signal transmission. PRS are defined for subcarrier spacing of 15 kHz only and are transmitted on antenna port six.
- CSI reference signals (CSI-RS): CSI reference signals are transmitted on antenna ports one, two, four or eight and are defined subcarrier spacing of 15 kHz only.
- MBSFN-specific reference signals (MBSFN-RS): MBSFN reference signals are transmitted only when the PMCH is transmitted. MBSFN-RS are defined for extended cyclic prefix only and are transmitted on antenna port four.

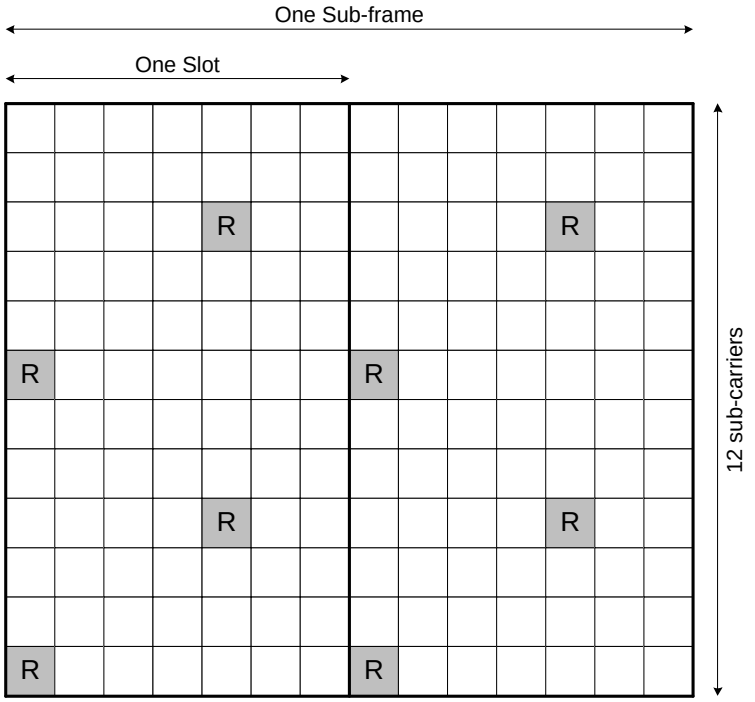

Figure 2.7 LTE Downlink Cell Specific Reference Signal [2]

CHAPTER 3

RADIO PROPAGATION MODELS AND WIRELESS CHANNEL CHARACTERISTICS

3.1 Introduction

The performance of any wireless communication systems is mainly governed by the wireless channel environment. As opposed to the predictable and static wired channel characteristics, the characteristics of a wireless channel is rather unpredictable and dynamic, which makes an exact analysis of the wireless communication system often difficult. In recent years, with the rapid growth of mobile communication services and emerging broadband mobile internet access services, optimization of the wireless communication system has become critical. Therefore, understanding of the wireless channels and correct knowledge of mobile fading channels is a necessary for the design of high performance and bandwidth efficient wireless communications systems.

In wireless communication system, the propagation of radio waves is mainly affected by three basic radio propagation mechanisms namely diffraction, reflection, and scattering. Diffraction occurs when the radio path between the transmitter and receiver is obstructed by a surface with sharp irregularities or small openings, appearing as a bending of waves around the small obstacles and openings. Reflection occurs when a radio wave propagating in one medium impinges upon another medium with different electromagnetic properties, for example, surface of the earth, buildings and walls. Scattering is the physical phenomenon in which the radiation of an electromagnetic wave is forced to deviate from a straight path by one or more localized obstacles, with small dimensions compared to the wavelength [4].

In addition to the additive noise which is the most common source of signal distortion, the wireless channel is significantly degraded by another phenomenon called fading. Fading is

referred to as the variation of the signal amplitude over time and frequency and can be broadly classified into two different types as large-scale fading and small-scale fading.

3.2 Large Scale Fading

Large-scale fading or long term fading occurs as the mobile moves through a very large distance. Path loss and shadowing are the two types of large scale fading that occur in a mobile communication system. Path loss is caused by loss of signal strength as a function of distance. The transmitted signal attenuates over distance since the energy of the signal is spread spherically around the transmitting antenna. Shadowing is a result of the loss of transmitted signal through absorption, reflection, scattering and diffraction by large objects such as buildings and trees along the path of the signal.

3.3 Small Scale Fading

Small-scale fading or short term fading is used to describe the rapid fluctuations of the signal amplitudes and phases due to the constructive and destructive interference of multiple signal paths of a radio signal over a short period of time or travel distances. Fading is caused by interference between two or more versions of the transmitted signal which arrive at the receiver at slightly different times called multipath. Depending on the relative extent of multipath delay spread, small-scaling fading is further classified as either frequency-selective fading or flat fading. Meanwhile, based on the Doppler spread, small-scaling fading is further classified as either fast fading or slow fading. Small scale fading is influenced by multipath propagation, speed of the mobile, speed of the surrounding objects and the transmission bandwidth of the signal. Figure 3.1 clearly shows the different fading components.

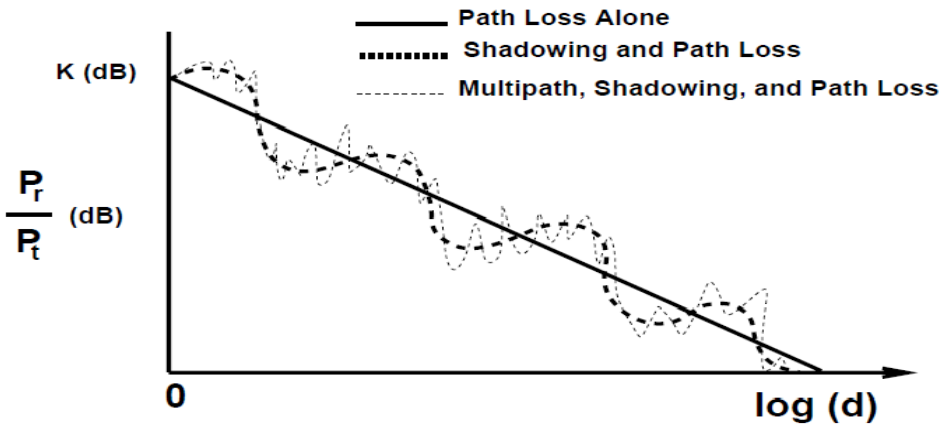

Figure 3.1 Path loss, shadowing and multipath fading [8]

3.3.1 Multipath Delay Spread and Coherence Bandwidth

Delay spread and coherence bandwidths are the parameters which describes the time dispersive nature of the channel. The power delay profile (PDP) specifies the characteristics of a multipath fading channel. The mean excess delay, root mean square (RMS) delay spread and excess delay spread are useful multipath channel parameters that can be determined from a PDP which can provide a reference to compare different multipath channels and to develop a general design guideline for wireless systems. If τ_k denotes the channel delay of the k^{th} path while a_k and $P(\tau_k)$ denote the amplitude and power respectively, then the mean excess delay ($\bar{\tau}$) is the first moment of the PDP and is defined as

$$\bar{\tau} = \frac{\sum_k a_k^2 \tau_k}{\sum_k a_k^2} = \frac{\sum_k P(\tau_k)\tau_k}{\sum_k P(\tau_k)} \tag{3.1}$$

The RMS delay spread (σ_τ) is the square root of the second central moment of the PDP and is defined as

$$\sigma_\tau = \sqrt{\overline{\tau^2} - (\bar{\tau})^2} \tag{3.2}$$

$where,$

$$\overline{\tau^2} = \frac{\sum_k a_k^2 \tau_k^2}{\sum_k a_k^2} = \frac{\sum_k P(\tau_k)\tau_k^2}{\sum_k P(\tau_k)} \quad (3.3)$$

The PDP and the magnitude frequency response or the spectral response of a wireless mobile radio channel is related through the Fourier transform. Similar to the delay spread parameters in the time domain, coherence bandwidth is used to characterize the channel in the frequency domain. The coherence bandwidth (B_C) is inversely proportional to the RMS delay spread and is defined as the range of frequencies over which channel behavior remains invariant and passes all spectral components with equal gain and linear phase.

A multipath channel can be categorized as either flat fading or frequency-selective fading depending on multipath delay spread and coherence bandwidth as follows:

Flat Fading - A channel is referred to as flat fading if the mobile radio channel has a constant gain and linear phase response over a bandwidth which is greater than the bandwidth of the transmit signal, i.e. the coherence bandwidth (B_C) is greater than the signal bandwidth (B_S). The delay spread (σ_τ) is smaller than the symbol period (T_S) and all the frequency components of the signal will experience the same amount of fading.

Frequency Selective Fading - A channel is referred to as frequency selective fading if the mobile radio channel has a constant gain and linear phase response over a bandwidth smaller than the bandwidth of the transmit signal, i.e. coherence bandwidth (B_C) is smaller than the signal bandwidth (B_S). The delay spread (σ_τ) is greater than the symbol period (T_S) and the different frequency components will undergo different amount of fading.

3.3.2 Doppler Spread and Coherence Time

Doppler spread and coherence time are the parameters which describes the frequency dispersive or the time varying nature of the channel. The Doppler spread arises due to the motion of mobile terminal. The range of frequencies over which the received Doppler spectrum is essentially non-zero is termed as Doppler spread (B_D) which is the measure of the spectral broadening caused by the time rate of change of the radio channel. Analogous to the PDP in

the time domain, the Doppler power spectrum gives the statistical power distribution of the channel for a signal transmitted at just one frequency. The Doppler frequency (f_d) depends on the relative velocity of the mobile and the angle of movement of the mobile relative to the base station. Coherence time (T_C) is the measure of the time duration over which the characteristics of the channel is essentially invariant. The coherence time is inversely proportional to the Doppler spread.

A multipath channel can be categorized as either slow fading or fast fading depending on Doppler spread and coherence time as follows:

Slow Fading - A channel is referred to as slow fading if the mobile radio channel variations are slower than the baseband signal variations, i.e. coherence time (T_C) is greater than the signal symbol period (T_S). The Doppler spread (B_D) is smaller than the signal bandwidth (B_S).

Fast Fading - A channel is referred to as fast fading if the mobile radio channel variations are faster than the baseband signal variations, i.e. coherence time (T_C) is smaller than the signal symbol period (T_S). The Doppler spread (B_D) is greater than the signal bandwidth (B_S).

3.4 Rayleigh & Ricean Fading Distributions

Rayleigh fading distribution is used to describe the statistical time varying nature of the received signal or the envelope of an individual multipath component. The Rayleigh distribution generally follows a non-line-of-sight (NLOS) distribution. The envelope of the sum of two quadrature Gaussian noise signal obeys a Rayleigh distribution. The Rayleigh function is shown in figure 3.2 (a). If σ is the RMS value of the received signal and σ^2 is the time average power of the received signal before envelope detection then the probability density function $f_r(r)$ of the Rayleigh distribution is given as

$$f_r(r) = \begin{cases} \frac{r}{\sigma^2} \exp\left(-\frac{r^2}{2\sigma^2}\right), & 0 \le r \le \infty \\ 0, & r < 0 \end{cases} \tag{3.4}$$

Ricean fading distribution is used to describe the nature of the received signal in case of line of sight (LOS) environment where a dominant signal arrives along with many weaker multipath signals. As the dominant component becomes weaker and fades away, the Ricean distribution degenerates to a Rayleigh distribution. The Ricean distribution is shown in figure 3.2 (b). If A denotes the peak amplitude of the dominant signal and $I_0(\cdot)$ is the modified Bessel function of first kind and zero order then the probability density function $f_r(r)$ of the Ricean distribution is given as

$$f_r(r) = \begin{cases} \frac{r}{\sigma^2}\exp\left(-\frac{r^2+A^2}{2\sigma^2}\right) I_0\left(\frac{Ar}{\sigma^2}\right), & A \geq 0, r \geq 0 \\ 0, & r < 0 \end{cases} \quad (3.5)$$

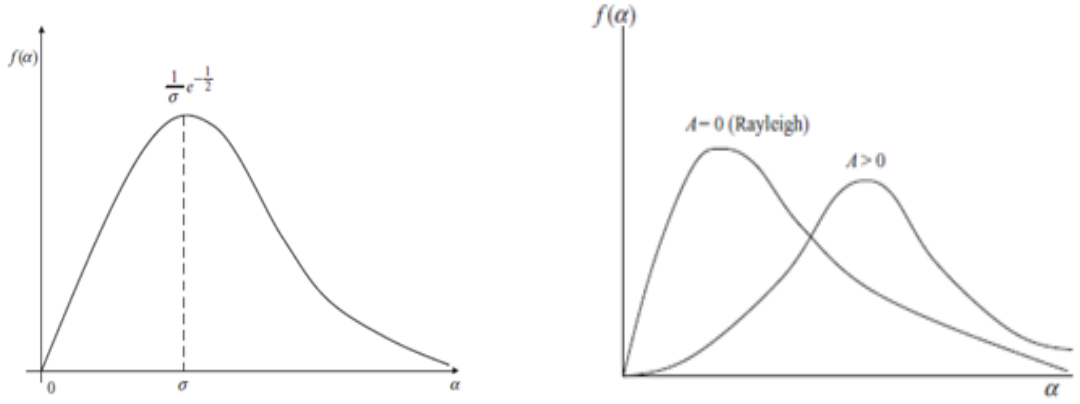

(a) (b)

Figure 3.2 (a) Rayleigh Distribution (b) Ricean Distribution [9]

3.5 Standard Wireless Channel Models

To simulate radio wave propagation, several wireless channel models exist and are currently used in the industry wherein each model is suitable for a certain type of environment. The ITU standard channel model specified in ITU-R recommendation M.1225 which were mainly used in the deployment of 3G 'IMT-2000' group of radio access systems have a structure

similar to the 3GPP multipath channel model. The ITU-R specifies three different test environments [11]:

- Indoor Office Test Environment – It is characterized by small cells and low transmit-powers with both base stations and pedestrian users located indoors. The type of fading is either Rayleigh or Ricean with Doppler frequency offsets depending on the walking speeds.
- Outdoor to Indoor and Pedestrian Test Environment – It is characterized by small cells and low transmit-powers with low antenna heights located outside and pedestrian users located on streets, inside buildings and residences. The type of fading is either Rayleigh or Ricean with Doppler frequency offsets depending on the walking speeds with occasional high fading rates due to reflections from moving vehicles.
- Vehicular Test Environment - It is characterized by large cells and high transmit-powers with higher cell capacity. The type of fading is either Rayleigh or Ricean with high fading rates due to fast moving vehicles.

For this thesis work, the ITU outdoor to indoor and pedestrian test environment is used. Table 3.1 gives the expected percentage of occurrence and the associated average RMS delay spread as specified in [11]. The tapped delay line parameters specifying the relative delays and average powers are illustrated in table 3.2, 3.3 and 3.4.

Table 3.1 Percentage of Occurrence and Associated Average RMS Delay Spread

Test Environment	Channel A		Channel B	
	r.m.s. (ns)	P (%)	r.m.s. (ns)	P (%)
Indoor Office	35	50	100	45
Outdoor to Indoor and Pedestrian	45	40	750	55
Vehicular	370	40	4000	55

Table 3.2 ITU Channel Model for Indoor Office Test Environment

Tap	Channel A		Channel B		Doppler Spectrum
	Relative Delay (ns)	Average Power (dB)	Relative Delay (ns)	Average Power (dB)	
1	0	0	0	0	Flat
2	50	-3.0	100	-3.6	Flat
3	110	-10.0	200	-7.2	Flat
4	170	-18.0	300	-10.8	Flat
5	290	-26.0	500	-18.0	Flat
6	310	-32.0	700	-25.2	Flat

Table 3.3 ITU Channel Model for Outdoor to Indoor and Pedestrian Test Environment

Tap	Channel A		Channel B		Doppler Spectrum
	Relative Delay (ns)	Average Power (dB)	Relative Delay (ns)	Average Power (dB)	
1	0	0	0	0	Classic
2	110	-9.7	200	-0.9	Classic
3	190	-19.2	800	-4.9	Classic
4	410	-22.8	1200	-8.0	Classic
5	-	-	2300	-7.8	Classic
6	-	-	3700	-23.9	Classic

Table 3.4 ITU Channel Model for Vehicular Test Environment

Tap	Channel A		Channel B		Doppler Spectrum
	Relative Delay (ns)	Average Power (dB)	Relative Delay (ns)	Average Power (dB)	
1	0	0	0	-2.5	Classic
2	310	-1.0	300	0	Classic
3	710	-9.0	8900	-12.8	Classic
4	1090	-10.0	12900	-10.0	Classic
5	1730	-15.0	17100	-25.2	Classic
6	2510	-20.0	20000	-16.0	Classic

CHAPTER 4

PILOT BASED CHANNEL ESTIMATION

4.1 Introduction

Channel estimation is an important part for the design of receivers in mobile communication systems. In order to recover the transmitted information correctly, the effect of the channel on the transmitted signal must be correctly estimated. Some of the channel models are described in chapter 3. The transmitted information can be precisely recovered by the receiver as long as it can keep track of the varying radio propagation channel statistics. The pilot based channel estimation methods are based on the pilot symbols which are transmitted along with the information signal. The pilot sequence or symbols are inserted into fixed positions of the transmitted signals so as to keep track of the varying radio channel statistics. The receiver has perfect knowledge of the pilot sequence and also the fixed pilot positions so that it can estimate the channel depending on the received pilot sequence.

In OFDM, as the subcarriers are orthogonal, each subcarrier component of the received signal can be expressed as the product of the transmitted signal and the channel frequency response at the respective subcarrier. In order to choose the proper channel estimation technique for the OFDM system, different factors such as the required performance, the channel variations in time and frequency domain and most importantly the computational complexity must be taken into account.

The pilot arrangements can either be of Block type or Comb type for one-dimensional (1D) channel estimation. Block type pilot arrangement based channel estimation is suitable for frequency selective fading channels and for slow fading channels. Comb type pilot arrangement based channel estimation is suitable for flat fading channels and for fast fading channels. Lattice

type pilot arrangement based channel estimation is used for two-dimensional (2D) channel estimation. It is suitable for channel estimation under any type of fading conditions.

4.2 Signal Model

For the purpose of channel estimation, the frequency response vectors of the input signal, received signal, channel and Gaussian noise (AWGN) vectors are used. The signal model used for the pilot based channel estimation is given by the following equation [21],

$$Y = XH + W = XFh + W \tag{4.1}$$

$where,$

$Y\ is\ the\ received\ output\ signal,$ $$Y = [Y(0)\ Y(1)\ \dots\dots\ Y(N-1)]^T \tag{4.2}$$

$X\ is\ the\ transmitted\ input\ signal,$ $$X = diag\{X(0), X(1), \dots, X(N-1)\} \tag{4.3}$$

$W\ is\ the\ AWGN\ noise,$ $$W = [W(0)\ W(1)\ \dots\dots W(N-1)]^T \tag{4.4}$$

$h\ is\ the\ channel\ impulse\ response,$ $$h = [h(0)\ h(1)\ \dots\dots h(N-1)]^T \tag{4.5}$$

$H\ is\ the\ channel\ frequency\ response,$ $$H = DFT_N(h) = Fh = [H(0)\ H(1)\ \dots\dots\ H(N-1)]^T \tag{4.6}$$

$F\ is\ the\ Fourier\ Transform\ Matrix,$ $$F = \begin{bmatrix} A_N^{00} & \cdots & A_N^{0(N-1)} \\ \vdots & \ddots & \vdots \\ A_N^{(N-1)0} & \cdots & A_N^{(N-1)(N-1)} \end{bmatrix};\ A_N^{nk} = \frac{1}{N}\, e^{-j2\pi\frac{n}{N}k} \tag{4.7}$$

4.3 Types of Pilot Arrangements

The different types of pilot arrangements along with the channel estimation techniques or methods used are described below.

4.3.1 Block Type Pilot Arrangement

In Block type of pilot arrangement, OFDM symbols with pilots at all subcarriers, referred to as pilot symbols are transmitted periodically for channel estimation. A time-domain interpolation along the time axis is performed using the pilots to estimate the channel. In order

to keep track of the time varying channel characteristics, the period of the pilot symbols in time or the pilot symbol period (S_t) must be such that it is less than the coherence time. As the coherence time is equivalent to the inverse form of the Doppler frequency (f_d), the pilot symbol period (S_t) must satisfy the following inequality [4]:

$$S_t \leq \frac{1}{f_d} \tag{4.8}$$

Block type pilot arrangement gives better performance for frequency selective channels as each pilot symbol contains known pilot signals at all of the subcarriers. However, this type of pilot arrangement is suitable only for slow fading channels. For fast fading channels, to keep track of the channel variations the pilot spacing must be reduced which increases the amount of overhead required to track the channel variations.

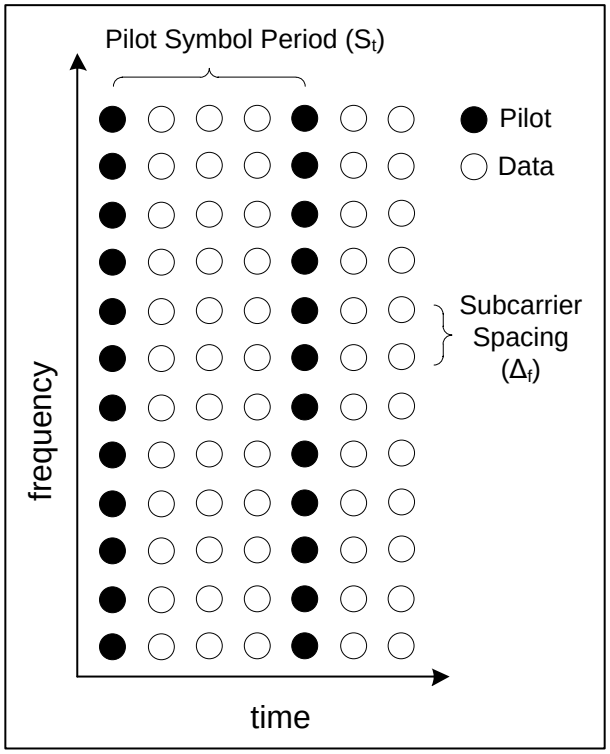

Figure 4.1 Block Type Pilot Arrangement

As the receiver knows the pilot symbol period (S_t), the channel is estimated at each pilot symbol. This estimated channel is used for the data OFDM symbols, until the next pilot symbol arrives for a slow fading channel. Figure 4.1 shows the Block type pilot arrangement.

4.3.2 Comb Type Pilot Arrangement

In Comb type of pilot arrangement, every OFDM symbol has (N_p) pilot tones which are periodically inserted into the input signal (X) with pilot subcarrier spacing (S_f). A frequency-domain interpolation along the frequency axis is performed using the pilots to estimate the channel. In order to keep track of the frequency-selective channel characteristics, the pilot subcarrier spacing (S_f) must be such that it is less than the coherence bandwidth. As the coherence bandwidth is equivalent to the inverse form of the maximum delay spread (σ_{max}), the pilot subcarrier spacing (S_f) must satisfy the following inequality [4]:

$$S_f \leq \frac{1}{\sigma_{max}} \tag{4.9}$$

Comb type pilot arrangement gives better performance for fast fading channels as each OFDM symbol contains known pilot signals at some of the subcarriers. However, this type of pilot arrangement is not suitable for frequency-selective channels. As the receiver knows the pilot locations for each OFDM symbol, it estimates the channel conditions at the pilot subcarriers which are then interpolated over the total subcarrier length (N) to get the overall channel frequency response at each OFDM symbol. As described above for Block type pilot arrangement, the same channel estimation techniques namely LS, MMSE and Modified MMSE channel estimation are used to estimate the channel response at the pilot subcarriers. It is then interpolated using different interpolation techniques to get the channel frequency response. Figure 4.2 shows the Comb type pilot arrangement.

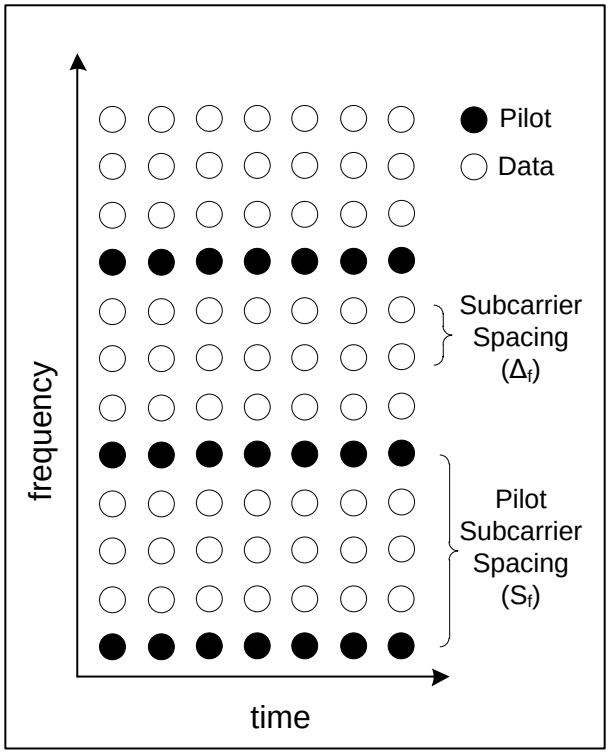

Figure 4.2 Comb Type Pilot Arrangement

4.3.3 Lattice Type Pilot Arrangement

In lattice type of pilot arrangement, pilots are inserted along both the time and the frequency axes for channel estimation. A frequency-domain interpolation along the frequency axis and a time domain interpolation along the time axis are performed using the pilots to estimate the channel. In order to keep track of the frequency-selective and the time varying channel characteristics, the pilot subcarrier spacing (S_f) must be less than the coherence bandwidth and the pilot symbol period (S_t) must be less than the coherence time. The pilot symbol arrangement must satisfy the following inequality [4]:

$$S_t \leq \frac{1}{f_d} \ and \ S_f \leq \frac{1}{\sigma_{max}} \tag{4.10}$$

Depending on the pilot arrangement and also the channel characteristics, lattice type pilot arrangement can be used to estimate the channel in case of both frequency selective as well as fast fading channels. Figure 4.3 shows the lattice type pilot arrangement.

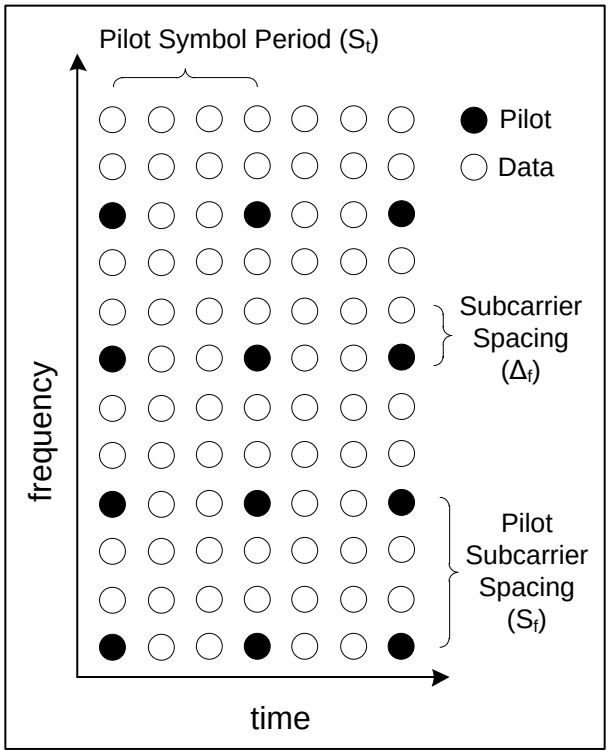

Figure 4.3 Lattice Type Pilot Arrangement

4.4 Channel Estimation for Block Type Pilot Arrangement

4.4.1 Least Square (LS) Channel Estimation

The least square (LS) channel estimation is a simple estimation technique with very low complexity. It does not require any prior knowledge of the channel statistics. It is widely used because of its simplicity. However, it suffers from a high mean square error. The LS estimation channel frequency response ($\widehat{H}_{LS}$) is obtained by minimizing the following cost function (J) without noise [4]:

$$\begin{aligned} J &= \left\| Y - X\hat{H} \right\|^2 \\ &= (Y - X\hat{H})^H (Y - X\hat{H}) \\ &= Y^H Y - Y^H X\hat{H} - \hat{H}X^H Y + \hat{H}^H X^H X\hat{H} \end{aligned} \quad (4.11)$$

$\hat{H} = Channel\ frequency\ response\ of\ the\ pilot\ OFDM\ symbol$

$(.)^H = conjugate\ transpose\ operation$

The LS estimated channel is obtained by setting the derivative of J with respect to $\hat{H}$ to zero,

$$\frac{\partial J}{\partial \hat{H}} = \ -Y^H X - X^H Y + 2\left(X^H X\hat{H}\right)^* = 0$$

$As\ X^H X\hat{H} = X^H Y,$

$\therefore \hat{H}_{LS} = (X^H X)^{-1} X^H Y = X^{-1} Y$

For each subcarrier (k) the LS estimated channel is given as,

$\hat{H}_{LS}[k] = Y[k]/X[k], \quad where\ k = 0,1,2, \ldots., N_{sc} - 1$

4.4.2 Minimum Mean Square Error (MMSE) Channel Estimation

The minimum mean square error (MMSE) channel estimation is an estimation technique with very high computational complexity. It requires prior knowledge of the second order channel statistics. The MMSE estimation channel frequency response ($\hat{H}_{MMSE}$) is obtained by minimizing the mean square error (e) between the actual channel (H) and the raw estimated channel ($\hat{H}$).

$$\begin{aligned} e &= H - \hat{H} \\ E\{|e|^2\} &= E\{\left|H - \hat{H}\right|^2\} \\ &= E\{(H - \hat{H})^H (H - \hat{H})\} \end{aligned} \quad (4.12)$$

$E\{\}\ is\ the\ expectation$

Since the channel and the AWGN noise can be assumed to be uncorrelated, the MMSE estimated channel can be given as,

$$\widehat{H}_{MMSE} = R_{HY} R_{YY}^{-1} Y \tag{4.13}$$

where,

R_{HY} *is the cross covariance matrix between* H *and* Y

R_{HH}, R_{YY} *is the auto covariance matrix of* H *and* Y *respectively*

σ_N^2 *is the noise variance,* $\sigma_N^2 = E\{|W(k)|^2\}$

In the above equation,

$$\begin{aligned} R_{HY} &= E\{HY^H\} \\ &= E\{H(HX+W)^H\} \\ &= E\{HH^H X^H + HW^H\} \\ &= E\{HH^H\} X^H + 0 \\ &= R_{HH} X^H \end{aligned} \tag{4.14}$$

$$\begin{aligned} R_{YY} &= E\{YY^H\} \\ &= E\{(HX+W)(HX+W)^H\} \\ &= E\{HXH^H X^H + HXW + WH^H X^H + WW^H\} \\ &= XE\{HH^H\} X^H + 0 + 0 + E\{WW^H\} \\ &= XR_{HH} X^H + \sigma_N^2 I_N \end{aligned} \tag{4.15}$$

Assuming that the channel statistics, namely the auto-covariance of the channel (R_{HH}) and the noise variance (σ_N^2) are known at the receiver, the MMSE estimated channel can be given as,

$$\begin{aligned} \widehat{H}_{MMSE} &= R_{HY} R_{YY}^{-1} Y \\ &= R_{HH} X^H (XR_{HH} X^H + \sigma_N^2 I_N)^{-1} X\widehat{H}_{LS} \\ \therefore \widehat{H}_{MMSE} &= R_{HH}(R_{HH} + \sigma_N^2 (XX^H)^{-1})^{-1} \widehat{H}_{LS} \end{aligned} \tag{4.16}$$

4.4.3 Modified Minimum Mean Square Error (M-MMSE) Channel Estimation

Though MMSE channel estimation yields a much better performance than LS channel estimation, it has very high computational complexity. It is observed from equation (4.16) that every time the input signal X changes, complex matrix inversion operation is required. Thus, a simplified MMSE estimation technique is studied in which the term $(XX^H)^{-1}$ in equation (4.16) is first replaced by its expectation $E\{(XX^H)^{-1}\}$. Assuming the same signal constellation on all the subcarriers and equal probability on all constellation points [26],

$$E\{(XX^H)^{-1}\} = E\left\{\left|\frac{1}{X_k}\right|^2\right\} I \tag{4.17}$$

$where,$

$I\ is\ the\ identity\ matrix$

$X_k\ is\ the\ constellation\ point\ depending\ on\ the\ type\ of\ modulation\ scheme$

$For\ QPSK\ modulation, the\ values\ of\ X_k\ are\ (\pm 1 \pm i)$

$For\ 16QAM\ modulation, the\ values\ of\ X_k\ are\ (\pm 1 \pm i), (\pm 3 \pm i), (\pm 1 \pm 3i), (\pm 3 \pm 3i)$

Defining the average SNR value as

$$\overline{SNR} = E\{|X_k|^2\}/\sigma_N^2 \tag{4.18}$$

Defining the term β as

$$\beta = E\{|X_k|^2\}E\{|1/X_k|^2\} \tag{4.19}$$

$where,$

$\beta\ is\ a\ constant\ depending\ only\ on\ the\ signal\ constellation$

$The\ value\ of\ \beta\ is\ 1\ for\ QPSK\ modulation\ and\ 17/9\ for\ 16QAM\ modulation$

Thus, the Modified MMSE estimated channel can be simplified to,

$$\hat{H}_{M-MMSE} = R_{HH}(R_{HH} + \frac{\beta}{\overline{SNR}} I)^{-1} \hat{H}_{LS} \tag{4.20}$$

The above Modified MMSE channel estimation equation can be further simplified using the singular value decomposition (SVD) [26]. Let us consider the SVD of the channel auto

covariance matrix R_{HH}

$$R_{HH} = UVU^H \tag{4.21}$$

$where,$

$U\ is\ a\ unitary\ matrix$

$V\ is\ a\ diagonal\ matrix\ with\ singular\ values\ \lambda_k\ such\ that\ \lambda_0 \geq \lambda_1 \geq \lambda_2 \geq \cdots \geq \lambda_{N-1} \geq 0$

Thus, the Modified MMSE equation after SVD is given as,

$$\widehat{H}_{M-MMSE} = UVU^H(\ UVU^H + \frac{\beta}{\overline{SNR}}I)^{-1}\widehat{H}_{LS} \tag{4.22}$$

$$\therefore \widehat{H}_{M-MMSE} = U\Delta U^H\widehat{H}_{LS} \tag{4.23}$$

$where,$

$$\Delta = V(\ V + \frac{\beta}{\overline{SNR}}I)^{-1} = \frac{\lambda_k}{\lambda_k + \frac{\beta}{\overline{SNR}}} \quad ; k = 0,1,2 \ldots N-1 \tag{4.24}$$

The SVD simplifies the matrix inverse calculation. Though there is a slight degradation in the performance of Modified MMSE channel estimation as compared to MMSE channel estimation, there is an overall reduction in the calculation complexity by a large factor.

4.5 Channel Estimation for Comb Type Pilot Arrangement

4.5.1 Least Square (LS) Channel Estimation

The Least Square (LS) channel estimation at the pilot subcarriers for Comb type pilot arrangement is given by the following equation,

$$\widehat{H}_{LS}^{p}(k) = \frac{Y_p}{X_p} = \frac{Y(kS_f)}{X(kS_f)} \quad ; k = 0,1, \ldots \ldots, N_p - 1 \tag{4.25}$$

$where,$

$S_f\ is\ the\ subcarrier\ spacing, \quad S_f = \frac{N}{N_p}$

X_p *is the transmitted signal with pilot symbols at locations* kS_f

Y_p *is the received signal with pilot symbols at locations* kS_f

The above estimated channel is then interpolated over the total subcarrier length (N) to get the Least Square estimated channel frequency response.

4.5.2 Minimum Mean Square Error (MMSE) Channel Estimation

The Minimum Mean Square Error (MMSE) channel estimation at the pilot subcarriers for Comb type pilot arrangement is given by the following equation,

$$\widehat{H}^{p}_{MMSE}(k) \quad = R_{HH}(R_{HH} + \sigma_N^2 (X_p {X_p}^H)^{-1})^{-1} \widehat{H}^{p}_{LS}(k) \qquad ; k = 0,1, \dots \dots, N_p - 1 \qquad (4.26)$$

where,

R_{HH} *is the auto covariance matrix of* H

σ_N^2 *is the noise variance,* $\sigma_N^2 = E\{|W(k)|^2\}$

The above estimated channel is then interpolated over the total subcarrier length (N) to get the MMSE estimated channel frequency response.

4.5.3 Modified Minimum Mean Square Error (M-MMSE) Channel Estimation

The Modified Minimum Mean Square Error (M-MMSE) channel estimation at the pilot subcarriers are given by the following equation,

$$\widehat{H}^{p}_{M-MMSE}(k) \quad = U \Delta U^H \widehat{H}^{p}_{LS}(k) \qquad ; k = 0,1, \dots \dots, N_p - 1 \qquad (4.27)$$

where U *is the unitary matrix and* Δ *is the same as defined in* 4.24

The above estimated channel is then interpolated over the total subcarrier length (N) to get the M-MMSE estimated channel frequency response.

4.6 Interpolation Methods for Comb Type Pilot Arrangement Based Channel Estimation

As mentioned above, the estimated channel over the pilot subcarriers are then interpolated to estimate the channel at data subcarriers. The different one dimensional (1D) interpolation techniques used are described in detail below.

4.6.1 Linear Interpolation (LI)

In Linear Interpolation algorithm, two successive or adjacent pilot subcarriers are used to determine the channel response for data subcarriers that are located in between the pilot signals. Using Linear Interpolation method, the estimated channel response for the data subcarrier $d, kS_f \leq d < (k+1)S_f$, is given by the following equation [21],

$$\begin{aligned} \widehat{H}_{LI}(d) &= \widehat{H}_{LI}\left(kS_f + l\right) \\ &= \left(1 - \frac{l}{S_f}\right)\widehat{H}_p(k) + \frac{l}{S_f}\widehat{H}_p(k+1) \\ &= \widehat{H}_p(k) + \frac{l}{S_f}\left(\widehat{H}_p(k+1) - \widehat{H}_p(k)\right) \quad ; 0 \leq l < S_f \end{aligned} \tag{4.28}$$

Linear interpolation has a low computational complexity and can also give better performance when the subcarriers are close to each other. For simulations, the LI method can be implemented using the '*interp1'* function in MATLAB with method defined as '*linear'*.

4.6.2 Spline Cubic Interpolation (SCI)

In Spline Cubic Interpolation algorithm, a smooth and continuous polynomial fitted to the given data points is produced. In this method, the transfer function of each subcarrier is approximated by a third order polynomial with respect to l/S_f. Using Spline Cubic Interpolation method, the estimated channel response for the data subcarrier $d, kS_f \leq d < (k+1)S_f$, is given by the following equation

$$\begin{aligned}\widehat{H}_{SCI}(d) &= \widehat{H}_{SCI}(kS_f + l) \\ &= \widehat{H}_{SCI}(kS_f + l) \quad ; 0 \le l < S_f \\ &= \alpha_1 \widehat{H}_p(k+1) + \alpha_0 \widehat{H}_p(k) + \alpha_1 S_f \widehat{H}'_p(k+1) - \alpha_0 S_f \widehat{H}'_p(k)\ ;\ k \\ &\qquad = 0,1,\dots\dots, N_p - 1\end{aligned} \tag{4.29}$$

$where,$

$\widehat{H}'_p(k)\ is\ the\ first\ order\ derivative\ of \widehat{H}_p(k),$

$$\alpha_1 = \frac{3(S_f - l)^2}{S_f^2} - \frac{2(S_f - l)^3}{S_f^3}$$

$$\alpha_0 = \frac{3l^2}{S_f^2} - \frac{2l^3}{S_f^3}$$

Spline Cubic Interpolation uses a higher order interpolation for better interpolation accuracy. However, the improvement in performance is not proven for all cases and for some cases Linear Interpolation can give better performance than SCI [22]. For simulations, the SCI method can be implemented using the '*interp1'* function in MATLAB with method defined as *'cubic'*.

4.6.3 Low Pass Interpolation (LPI)

In Low Pass Interpolation algorithm, zeros are inserted into the original estimated channel $\widehat{H}_p(k)$ at the pilot subcarriers and then a low pass finite length impulse response (FIR) filter is applied to it, which allows the original data to pass through unchanged [23]. In this method, the mean square error between the interpolated points and their ideal values is minimized. For simulations, the LPI method can be implemented using the '*interp'* function in MATLAB.

CHAPTER 5

SIMULATIONS AND RESULTS

5.1 Introduction

The performance of different channel estimation schemes for the 3GPP LTE downlink 5 MHz bandwidth configuration has been evaluated and compared in this section in terms of BER for different SNR values. The 5 MHz bandwidth configuration parameters are specified in table 2.1 (a). The ITU channel model for outdoor to indoor and pedestrian test environment (Channel A) as described in chapter 3 is chosen in order to perform all the simulations. The FFT/IFFT size of 512 is used with CP length of 36 samples. The un-coded SISO system with QPSK modulation is considered for the thesis work. The Doppler frequency of 10 Hz is considered for the different pilot based channel estimation schemes. The sampling frequency is 7.68 MHz for all simulation.

5.2 Performance Analysis for Block Type Pilot Arrangement

For Block type pilot arrangement, the performance of LS channel estimation is compared with MMSE channel estimation algorithm. The pilot symbol period ($S_t = 7$) is used for simulation. It is observed that for MMSE channel estimation there is 5-6 dB improvement in performance for low SNR values and up to 3 dB for high SNR values as compared to LS channel estimation. The figure 5.1 shows the performance of LS and MMSE channel estimation scheme for Block type pilot arrangement.

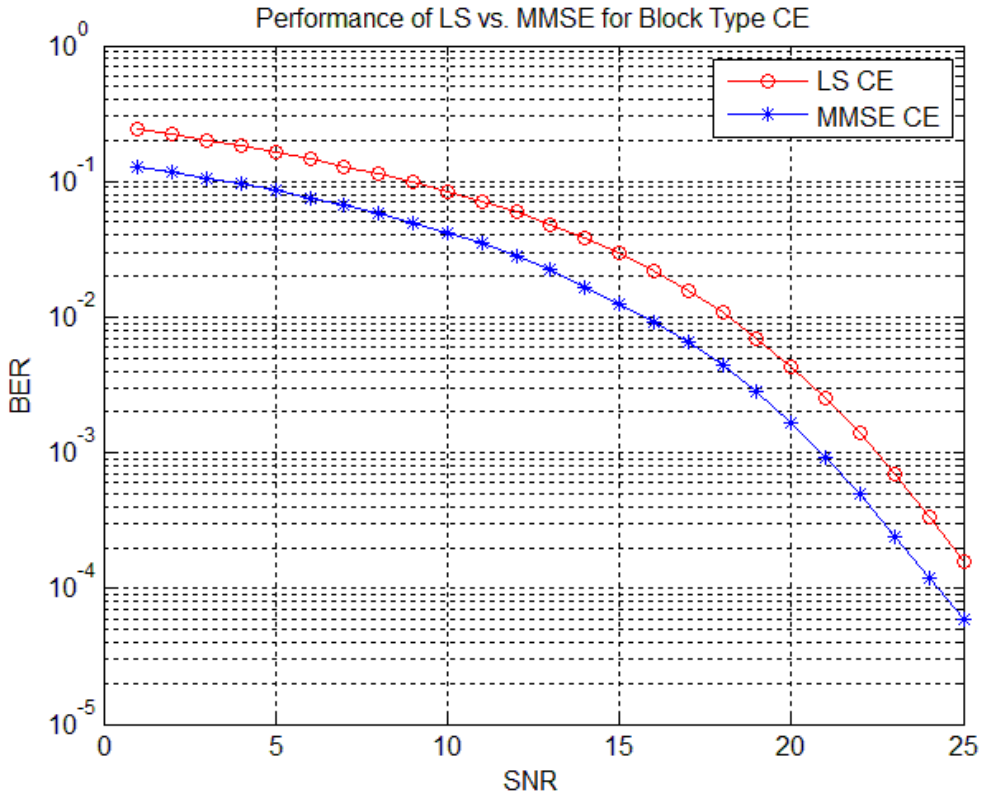

Figure 5.1 Performance of LS vs. MMSE for Block Type Pilot Arrangement

Next, the performance of Modified-MMSE channel estimation scheme is evaluated. It is observed that the Modified-MMSE channel estimation has better performance than LS channel estimation scheme. Also, its performance is comparable to that of MMSE with only a slight reduction in performance, close to 0.5 dB. The Modified-MMSE estimation algorithm however has a much lower computational complexity than MMSE and hence is preferred over MMSE for some real world applications. Figure 5.2 compares the performance of the three different channel estimation schemes.

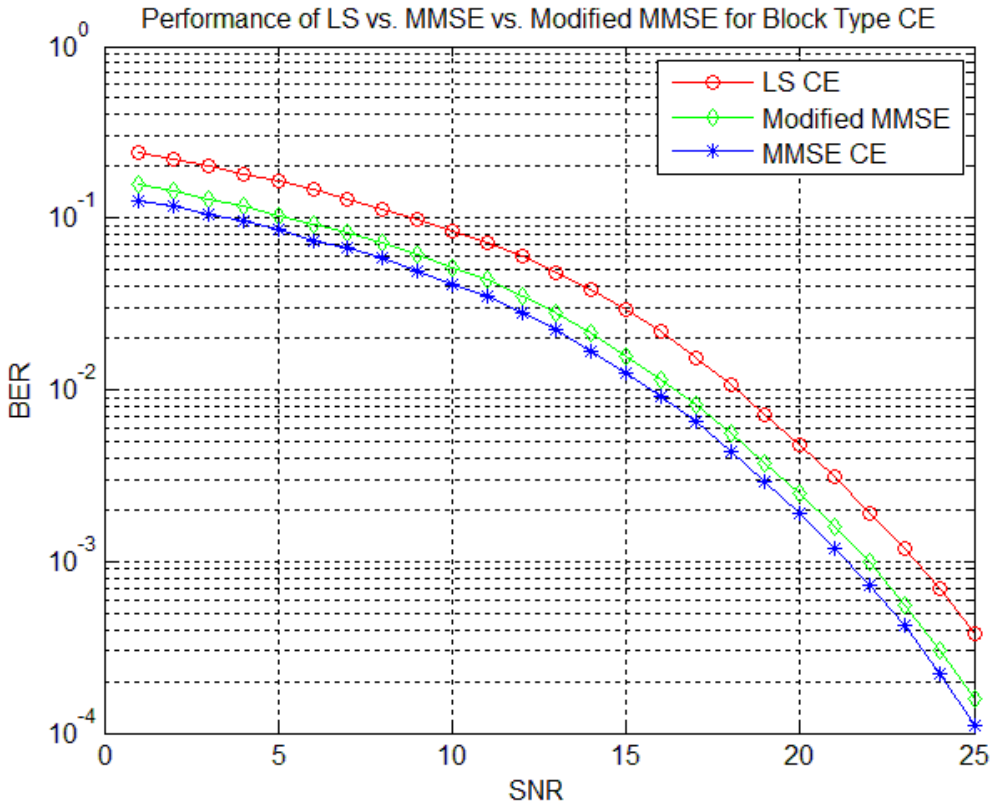

Figure 5.2 Performance of LS vs. MMSE vs. Modified MMSE for Block Type Pilot Arrangement

5.3 Performance Analysis for Comb Type Pilot Arrangement

For Comb type pilot arrangement, first the performance of LS channel estimation is compared with MMSE channel estimation algorithm with Linear Interpolation. The pilot subcarrier spacing ($S_f = 6$) is used for simulation. It is observed that for MMSE channel estimation there is 3-4 dB improvement in performance as compared to LS channel estimation. The figure 5.3 shows the performance of LS and MMSE channel estimation scheme for Comb type pilot arrangement with Linear Interpolation.

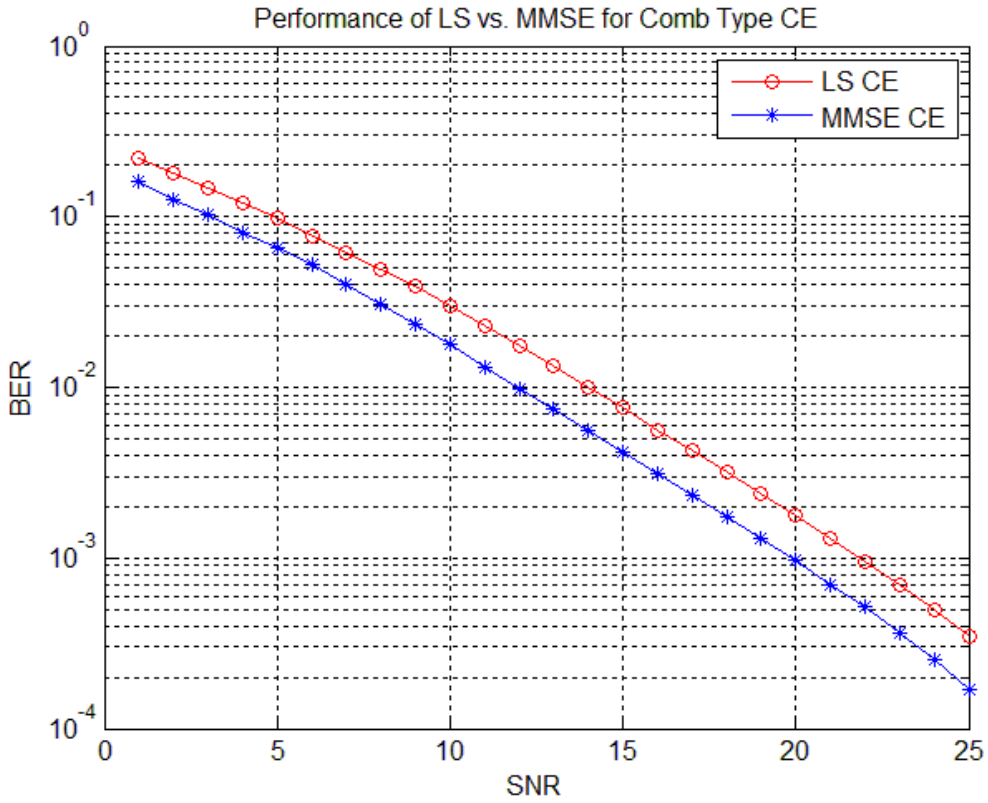

Figure 5.3 Performance of LS vs. MMSE for Comb Type Pilot Arrangement

Next, the performance of Modified-MMSE channel estimation scheme is evaluated for Comb type pilot arrangement with Linear Interpolation. It is observed that the Modified-MMSE channel estimation has better performance than LS channel estimation scheme. Also, its performance is comparable to that of MMSE with only a slight reduction in performance, close to 0.5 dB. The Modified-MMSE estimation algorithm however has a much lower computational complexity than MMSE and hence is preferred over MMSE for some real world applications. Figure 5.4 compares the performance of the three different channel estimation schemes for Comb type pilot arrangement with Linear Interpolation.

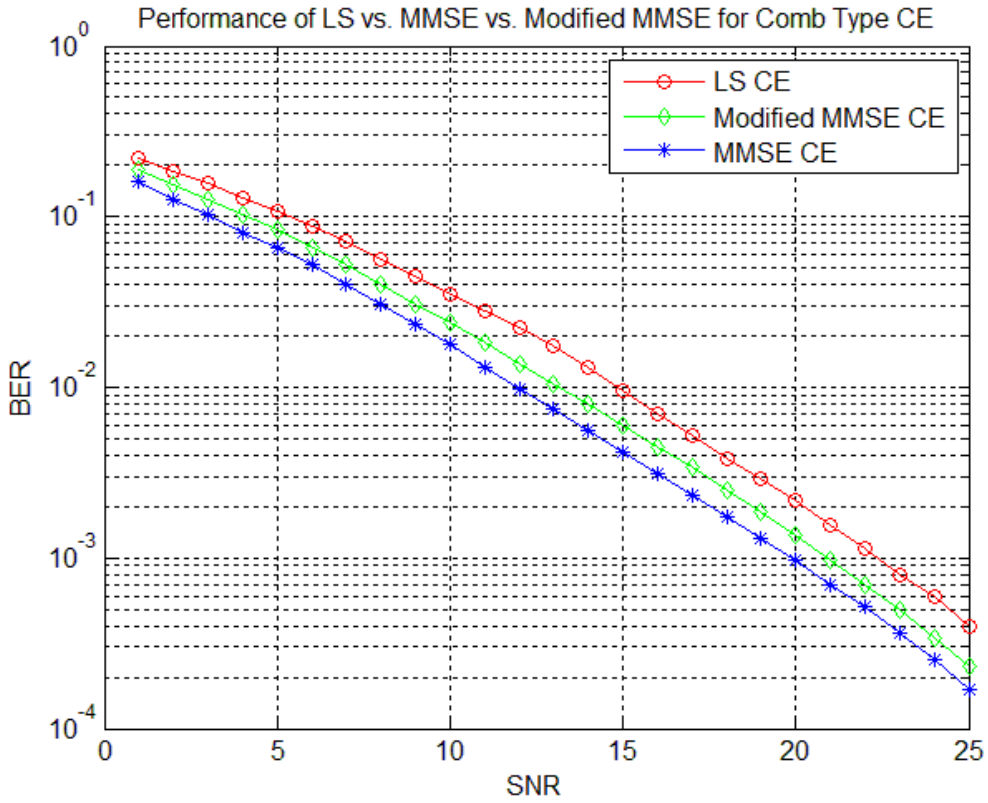

Figure 5.4 Performance of LS vs. MMSE vs. Modified MMSE for Comb Type Pilot Arrangement

Next, the performance of the different interpolation methods for Comb type pilot arrangement is evaluated. It is observed that Linear Interpolation gives the best performance. The performance of LPI is much better than SCI method and is close to that of LI. The performance of the interpolation method depends on many factors including the pilot subcarrier spacing, the channel characteristics and also the signal to noise ratio. Hence, though SCI uses higher order interpolation for better interpolation accuracy, the improvement in performance is not proven for all cases and for some cases Linear Interpolation can give better performance. For cases when the subcarrier spacing is very small compared to the coherence bandwidth, Linear Interpolation can give better performance in terms of BER [22]. Figure 5.5 shows the performance of the different interpolation methods with LS channel estimation.

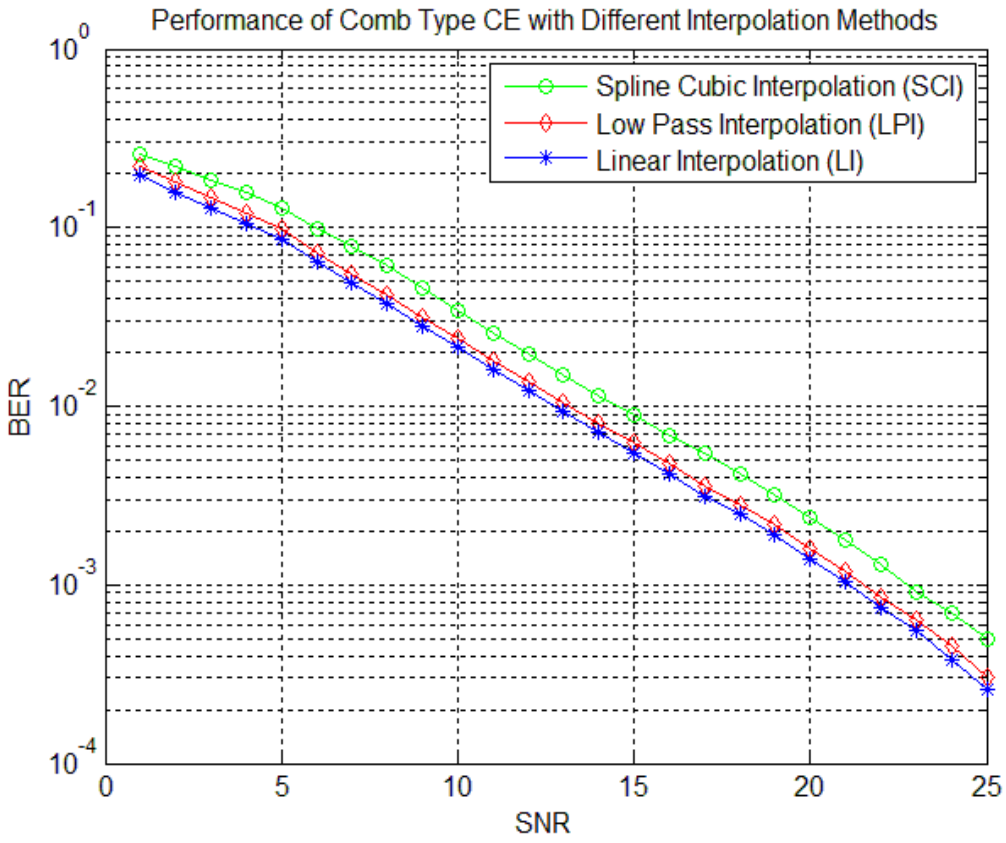

Figure 5.5 Performance of Comb Type with Different Interpolation Methods

Lastly, the performance for different pilot spacing over a PRB has been evaluated and it is seen that as the pilot spacing decreases, the performance of the system slowly improves. LS channel estimation method with Linear Interpolation is used for all the different pilot spacing arrangement. The performance is best for pilot subcarrier spacing ($S_f = 3$) and is the worst for pilot subcarrier spacing ($S_f = 12$). However, decreasing the pilot subcarrier spacing increases the no. of pilot subcarriers, thus reducing the number of data subcarriers which ultimately reduces the overall efficiency of the system in terms of useful data sent. Hence, the number of pilot subcarriers must be optimally selected. Figure 5.6 shows the performance of Comb type pilot arrangement for different pilot subcarrier spacing.

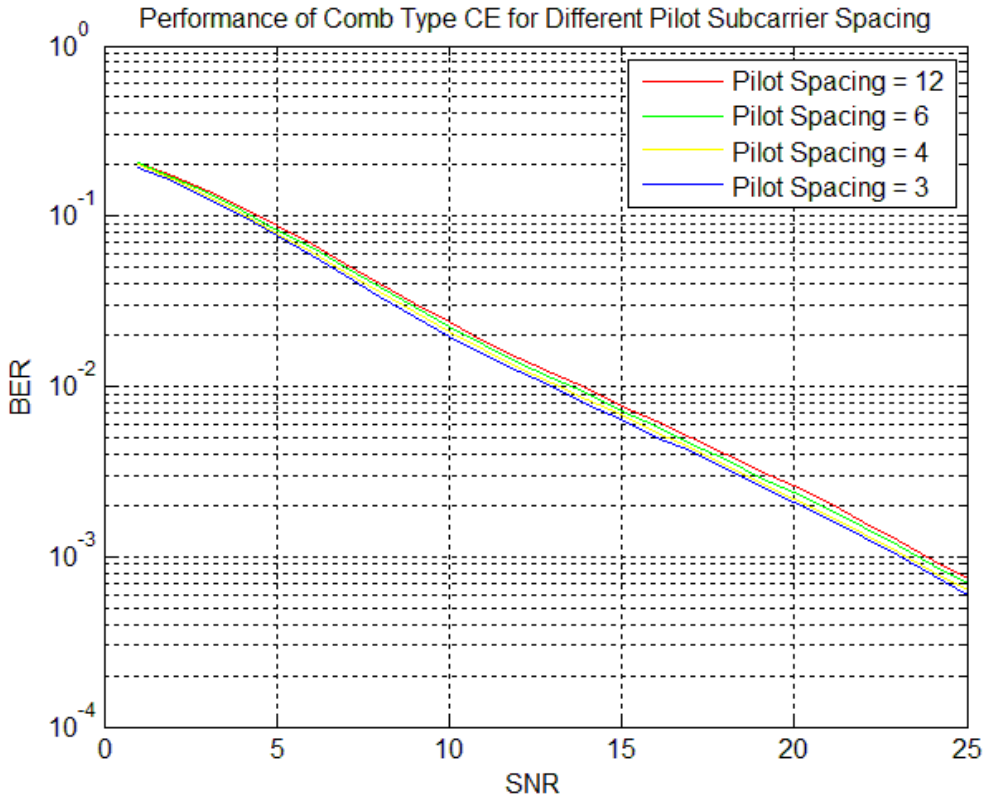

Figure 5.6 Performance of Comb Type for Different Pilot Subcarrier Spacing

CHAPTER 6

CONCLUSION AND FUTURE WORK

6.1 Conclusion

The purpose of this thesis work is to study the 3GPP LTE downlink specifications and to evaluate and compare the performance of different channel estimation schemes. The ITU channel model for outdoor to indoor and pedestrian test environment is chosen in order to perform realistic simulations for multipath fading and time varying channel characteristics. The 5 MHz bandwidth configuration for LTE downlink specification has been used for all simulations. The un-coded SISO system with QPSK modulation is considered for the thesis work.

The performance of different 1-D channel estimation schemes in terms of BER for different SNR values is evaluated. It is observed that MMSE channel estimation gives a better performance than LS channel estimation for both Block type and Comb type pilot arrangement. The Modified MMSE channel estimation shows to have a slight degradation in performance than MMSE but with a much lower computational complexity and hence can be preferred over MMSE for some real world applications. The different interpolation techniques are further investigated for Comb type pilot arrangement. It is observed that LI gives better performance than SCI and LPI method for the specified channel characteristics and pilot spacing. The performance for different pilot spacing is also studied and it is seen that as the pilot spacing decreases, the performance of the overall system slowly improves. However, decreasing the pilot subcarrier spacing increases the no. of pilot subcarriers. This ultimately results in less number of data subcarriers which is not desired. Hence, the number of pilot subcarriers must be optimally selected.

6.1 Future Work

Firstly, the current thesis work can be extended to evaluate the performance for different bandwidth configurations. For each bandwidth configuration, the different modulation schemes can be used and the performance for the same can be evaluated and compared. Also channel coding as well as MIMO can be added to the system for further implementation. Later, the performance for different 2-D pilot arrangement based channel estimation schemes can be studied.

APPENDIX A

ACRONYMS

3GPP	Third Generation Partnership Project
AMC	Adaptive Modulation and Coding
ARQ	Automatic Repeat Request
AWGN	Additive White Gaussian Noise
BER	Bit Error Rate
BS	Base Station
CE	Channel Estimation
CP	Cyclic Prefix
CRS	Cell Specific Reference Signals
CSI	Channel State Information
DFT	Discrete Fourier transform
DL	Downlink
DwPTS	Downlink Pilot Time Slot
EPS	Evolved Packet System
E-UTRAN	Evolved UTRAN
FDD	Frequency Division Duplex
FDM	Frequency Division Multiplexing
FDMA	Frequency Division Multiple Access
FFT	Fast Fourier transform
GP	Guard Period
HSDPA	High Speed Downlink Packet Access
HSPA	High Speed Packet Access
ICI	Inter Carrier Interference
IDFT	Inverse Discrete Fourier Transform
IFFT	Inverse Fast Fourier Transform
ISI	Inter Symbol Interference
ITU	International Telecommunication Union
LI	Linear Interpolation
LOS	Line of Sight
LPI	Low Pass Interpolation
LS	Least Square
LTE	Long Term Evolution
MIMO	Multiple Input Multiple Output
M-MMSE	Modified Minimum Mean Square Error
MMSE	Minimum Mean Square Error
NLOS	No Line of Sight
OFDM	Orthogonal Frequency Division Multiplexing
OFDMA	Orthogonal Frequency Division Multiple Access

OPEX	Operational Expenditure
PAPR	Peak to Average Power Ratio
PBCH	Physical Broadcast Channel
PCFICH	Physical Control Format Indicator Channel
PDCCH	Physical Downlink Control Channel
PDP	Power Delay Profile
PDSCH	Physical Downlink Shared Channel
PHICH	Physical Hybrid ARQ Indicator Channel
PMCH	Physical Multicast Channel
PRACH	Physical Random Access Channel
PRB	Physical Resource Block
PRS	Positioning Reference Signals
PUCCH	Physical Uplink Control Channel
PUSCH	Physical Uplink Shared Channel
QAM	Quadrature Amplitude Modulation
QoS	Quality of Service
QPSK	Quadrature Phase Shift Key
RAN	Radio Access Network
RE	Resource Element
RMS	Root Mean Square
SAE	System Architecture Evolution
SC-FDMA	Single Carrier Frequency Division Multiple Access
SCI	Spline Cubic Interpolation
SISO	Single Input Single Output
SM	Spatial Multiplexing
SON	Self-Optimizing Networks
SVD	Singular Value Decomposition
TD	Transmit Diversity
TDD	Time Division Duplex
TTI	Transmission Time Interval
UE	User Equipment
UL	Uplink
UMTS	Universal Mobile Telecommunications Systems
UpPTS	Uplink Pilot Time Slot
UTRAN	UMTS Terrestrial Radio Access Network

REFERENCES

[1] 3GPP, Release 8 V0.2.3, “Overview of 3GPP Release 8”, Release 8, June 2011

[2] 3GPP, TS 36.211 V10.2.0, “Physical Channels and Modulation”, Release 10, June 2011

[3] Stefania Sesia, Issam Toufik and Matthew Baker, “LTE - The UMTS Long Term Evolution: From Theory to Practice”, John Wiley & Sons Ltd, 2009

[4] Yong Soo Cho, Jaekwon Kim, Won Young Yang and Chung G. Kang, “MIMO-OFDM Wireless Communications with MATLAB”, John Wiley & Sons (Asia) Pte Ltd, 2010

[5] Borko Furht and Syed A. Ahson, “Long Term Evolution: 3GPP LTE Radio and Cellular Technology”, Taylor & Francis Group, Auerbach Publications, 2009

[6] Harri Holma and Antti Toskala, “LTE for UMTS-OFDMA and SC-FDMA based radio access”, John Wiley & Sons Ltd, 2009

[7] B. Walke, P. Seidenberg and M.P. Althoff, “UMTS: The Fundamentals”, John Wiley & Sons Ltd, 2003

[8] Andrea Goldsmith, “Wireless Communications”, Cambridge University Press, 2005

[9] Mischa Schwartz, “Mobile Wireless Communications”, Cambridge University Press, 2005

[10] Theodore Rappaport, “Wireless Communications: Principles and Practice”, 2nd Edition, Prentice Hall, 2002

[11] Recommendation ITU-R M.1225, “Guidelines for Evaluation of Radio Transmission Technologies for IMT-2000”, 1997

[12] Jim Zyren, “Overview of the 3GPP Long Term Evolution Physical Layer”, Freescale

[13] Adel A.M. Saleh and Reinaldo A. Valenzuela, “A Statistical Model for Indoor Multipath Propagation”, IEEE Journal on Selected Areas in Communications, Vol. SAC-5, No.2, February 1987

[14] Freescale Semiconductors, “Long Term Evolution Protocol Overview”, Document

Number: LTEPTCLOVWWP, October 2008

[15] Hyung G. Myung, “Technical Overview of 3GPP LTE”, May 2011

[16] 3GPP, TS 36.300 V10.5.0, “E-UTRA and E-UTRAN Overall Description”, Stage 2, Release 10, September 2011

[17] 3GPP, TR 25.892 V6.0.0, “Feasibility Study for Orthogonal Frequency Division Multiplexing (OFDM) for UTRAN Enhancement”, Release 6, 2006

[18] Michele Morelli and Umberto Mengali, “A Comparision of Pilot-Aided Channel Estimation Methods for OFDM Systems”, IEEE Transactions on Signal Processing, Vol. 49, No. 12, December 2001

[19] Meng-Han Hsieh and Che-Ho-Wei, “Channel Estimation for OFDM Systems based on Comb-type Pilot Arrangement in Frequency Selective Fading Channels”, IEEE Transactions on Consumer Electronics, Vol. 44, No. 1, February 1998

[20] Yushi Shen and Ed Martinez, “Channel Estimation in OFDM Systems”, Application Note AN3059, Freescale Semiconductor, 2006

[21] Sinem Coleri, Mustafa Ergen, Anuj Puri and Ahmad Bahai, “Channel Estimation Techniques Based on Pilot Arrangement in OFDM Systems”, IEEE Transactions on Broadcasting, Vol. 48, No. 3, September 2002

[22] David Bueche, Patrick Corlay and Marc Gazalet, “A method for Analyzing the Performance of Comb-type Pilot-aided Channel Estimation in Power Line Communications”, IEEE Transactions on Consumer Electronics, Vol. 54, No. 3, August 2008

[23] Hala M. Mahmoud, Allam S. Mousa and Rashid Saleem, “Channel Estimation Based in Comb-type Pilots Arrangement for OFDM System over Time Varying Channel”, Journal of Networks, Vol. 5, No. 7, July 2010

[24] Mahmut Yalcin, Aydin Akan and Hakan Dogan, “Channel Estimation for OFDM Systems with High Mobility Fading Channels”, Ultra Modern Telecommunications & Workshops,

ICUMT'09, October 2009

[25] Ove Edfors, Magnus Sandell, Jan-Jaap van de Beek, Sarah Kate Wilson and Per Ola Borjesson, "OFDM Channel Estimation by Singular Value Decomposition", IEEE Transactions on Communications, Vol. 46, No. 7, July 1998

[26] 3GPP, TS 36.213 V10.2.0, "E-UTRA Physical Layer Procedures", Release 10, June 2011

[27] Steven M. Kay, "Fundamentals of Statistical Signal Processing: Detection Theory", Volume II, Prentice Hall PTR, 1998

[28] Shigenori Kinjo, "A new MMSE channel estimation algorithm for OFDM systems", IEICE Electronics Express, Vol. 5, No. 18, 738-743

[29] Steven M. Kay, "Fundamentals of Statistical Signal Processing: Estimation Theory", PTR Prentice Hall, Englewood Cliffs, New Jersey, 1993

[30] Yang Qin, Bing Hui and Kyung Hi Chang, "Performance and Complexity Evaluation of Pilot Based Channel Estimation Algorithms for 3GPP LTE Downlink", Ubiquitous and Future Networks (ICUFN), 2010 Second International Conference on , vol., no., pp.218-221, 16-18, June 2010

[31] John G Proakis, "Digital Communications", Fourth Edition, McGraw Hill, August 2000

[32] Ye (Geoffrey) Li, "Pilot Symbol Aided Channel Estimation for OFDM in wireless Systems", IEEE Transactions on vehicular technology, Vol. 49, No. 4, July 2000

BIOGRAPHICAL INFORMATION

Ankit Ashok Agarwal was born in Sonapur, India in September 1985. He received his Bachelor's of Engineering (B.E.) degree in Electronics and Telecommunications from Pune University, India in 2008. He later joined the University of Texas at Arlington in Spring 2010 to pursue a Master of Science degree in Electrical Engineering. His interests are in wireless communications, digital communication and embedded microcontroller system design.